

UNCLASSIFIED

**BRAKE FLUID COMPATIBILITY STUDIES WITH
ADVANCED BRAKE SYSTEMS**

**INTERIM REPORT
TFLRF No. 473**

**By
Douglas M. Yost
Nigil Jeyashekar
Edwin A. Frame**

**U.S. Army TARDEC Fuels and Lubricants Research Facility
Southwest Research Institute[®] (SwRI[®])
San Antonio, TX**

**For
Zackery J. Schroeder
U.S. Army TARDEC
Force Projection Technologies
Warren, Michigan**

Contract No. W56HZV-09-C-0100 (WD34)

UNCLASSIFIED: Distribution Statement A. Approved for public release

January 2016

UNCLASSIFIED

Disclaimers

Reference herein to any specific commercial company, product, process, or service by trade name, trademark, manufacturer, or otherwise, does not necessarily constitute or imply its endorsement, recommendation, or favoring by the United States Government or the Department of the Army (DoA). The opinions of the authors expressed herein do not necessarily state or reflect those of the United States Government or the DoA, and shall not be used for advertising or product endorsement purposes.

Contracted Author

As the author(s) is (are) not a Government employee(s), this document was only reviewed for export controls, and improper Army association or emblem usage considerations. All other legal considerations are the responsibility of the author and his/her/their employer(s).

DTIC Availability Notice

Qualified requestors may obtain copies of this report from the Defense Technical Information Center, Attn: DTIC-OCC, 8725 John J. Kingman Road, Suite 0944, Fort Belvoir, Virginia 22060-6218.

Disposition Instructions

Destroy this report when no longer needed. Do not return it to the originator.

UNCLASSIFIED

BRAKE FLUID COMPATIBILITY STUDIES WITH ADVANCED BRAKE SYSTEMS

**INTERIM REPORT
TFLRF No. 473**

**By
Douglas M. Yost
Nigil Jeyashekar
Edwin A. Frame**

**U.S. Army TARDEC Fuels and Lubricants Research Facility
Southwest Research Institute[®] (SwRI[®])
San Antonio, TX**

**For
Zackery J. Schroeder
U.S. Army TARDEC
Force Projection Technologies
Warren, Michigan**

**Contract No. W56HZV-09-C-0100 (WD34)
SwRI[®] Project No. 08.20680**

UNCLASSIFIED: Distribution Statement A. Approved for public release

January 2016

Approved by:



**Gary B. Bessee, Director
U.S. Army TARDEC Fuels and Lubricants
Research Facility (SwRI[®])**

UNCLASSIFIED

UNCLASSIFIED

UNCLASSIFIED

REPORT DOCUMENTATION PAGE			<i>Form Approved</i> <i>OMB No. 0704-0188</i>		
Public reporting burden for this collection of information is estimated to average 1 hour per response, including the time for reviewing instructions, searching existing data sources, gathering and maintaining the data needed, and completing and reviewing this collection of information. Send comments regarding this burden estimate or any other aspect of this collection of information, including suggestions for reducing this burden to Department of Defense, Washington Headquarters Services, Directorate for Information Operations and Reports (0704-0188), 1215 Jefferson Davis Highway, Suite 1204, Arlington, VA 22202-4302. Respondents should be aware that notwithstanding any other provision of law, no person shall be subject to any penalty for failing to comply with a collection of information if it does not display a currently valid OMB control number. PLEASE DO NOT RETURN YOUR FORM TO THE ABOVE ADDRESS.					
1. REPORT DATE (DD-MM-YYYY) 16-JAN 2015		2. REPORT TYPE Interim Report		3. DATES COVERED (From - To) September 2014 – January 2016	
4. TITLE AND SUBTITLE Brake Fluid Compatibility Studies with Advanced Brake Systems			5a. CONTRACT NUMBER W56HZV-09-C-0100		
			5b. GRANT NUMBER		
			5c. PROGRAM ELEMENT NUMBER		
6. AUTHOR(S) Yost, Douglas; Jeyashekar, Nigil; Frame, Edwin			5d. PROJECT NUMBER SwRI 08.20680		
			5e. TASK NUMBER WD 34		
			5f. WORK UNIT NUMBER		
7. PERFORMING ORGANIZATION NAME(S) AND ADDRESS(ES) U.S. Army TARDEC Fuels and Lubricants Research Facility (SwRI®) Southwest Research Institute® P.O. Drawer 28510 San Antonio, TX 78228-0510			8. PERFORMING ORGANIZATION REPORT NUMBER TFLRF No. 473		
9. SPONSORING / MONITORING AGENCY NAME(S) AND ADDRESS(ES) U.S. Army RDECOM U.S. Army TARDEC Force Projection Technologies Warren, MI 48397-5000			10. SPONSOR/MONITOR'S ACRONYM(S)		
			11. SPONSOR/MONITOR'S REPORT NUMBER(S)		
12. DISTRIBUTION / AVAILABILITY STATEMENT UNCLASSIFIED: Dist A Approved for public release; distribution unlimited					
13. SUPPLEMENTARY NOTES					
14. ABSTRACT A prior study with MIL-PRF-46176 silicone brake fluid and SAE J1703 DOT 3 brake fluid in a hydraulic power brake system revealed deposits only with the silicone brake fluid after 20,000-cycles of testing. These results are published in Interim Report TFLRF no. 445. The overall conclusion is that the root cause of deposit buildup in the system reservoir, that caused testing with silicone brake fluid to halt in FY13, is due to formation of a thin Styrene-Butadiene (SBR) elastomer residue on the servo valves. This conclusion has been substantiated through a number of conclusions from static soak and dynamic seal tests, followed by a series of conclusions from physical and chemical characterization tests. Increased wear seen with the silicone brake fluid on brake system parts was substantiated by laboratory bench wear tests of the brake fluids.					
15. SUBJECT TERMS Brake Fluid, SAE J1703, MIL-PRF-46176, FTIR, elastomer, lubricity, BOCLE, HFRR					
16. SECURITY CLASSIFICATION OF:			17. LIMITATION OF ABSTRACT	18. NUMBER OF PAGES	19a. NAME OF RESPONSIBLE PERSON
a. REPORT Unclassified	b. ABSTRACT Unclassified	c. THIS PAGE Unclassified	Unclassified	72	19b. TELEPHONE NUMBER (include area code)

EXECUTIVE SUMMARY

The objective of this work was to determine the root cause of deposit buildup in the brake system reservoir that caused testing with silicone brake fluid to be halted in a prior study with MIL-PRF-46176 silicone brake fluid and SAE J1703 DOT 3 brake fluid in a hydraulic power brake system. The study results published in Interim Report TFLRF no. 445, revealed deposits formed only with the silicone brake fluid after 20,000-cycles of testing. The objective was accomplished by conducting static soak tests and dynamic seal tests, followed by a series of physical and chemical characterization tests on used silicone brake fluid and hydraulic pressure brake test system components, in an effort to determine the identity and cause of the deposit buildup.

Static soak tests of four different elastomers with silicone brake fluid was conducted at ambient and 40 °C, primarily to determine using GC-MS, if the chemical constituents in the silicone brake fluid caused elastomer dissolution into the silicone brake fluid. Due to absence of elastomer based compounds in the used fluid from the static soak tests, based on GC-MS data, it was concluded that silicone brake fluid did not cause elastomer dissolution at ambient conditions and at 40 °C. This was followed by conducting dynamic seal tests to determine if wear due to dynamic motion would have caused elastomer dissolution into the silicone brake fluid. This aspect was judged by looking at the percentage increase in thickness between pre-test and post-test measurements. As the elastomer absorbs sufficient brake fluid causing it to swell, it increases the thickness causing the elastomer to squeeze against the moving or sliding surface resulting in elastomer wear and dissolution into the fluid. The results from the dynamic seal tests indicated that Neoprene, Silicone and EPDM elastomers have either no change or decrease in thickness, while SBR elastomer had about 6% increase in thickness. This increases elastomer squeeze creating circumstances for elastomer wear and dissolution during dynamic motion.

The eleven elastomer seals from various Hydraulic Pressure Brake (HPB) components were identified using FTIR. The identity of the Parking Brake Supply and Relay Valve Seal remains unclear due to proprietary nature of the filter combinations used in the elastomer; could be either

EPDM or SBR. Similarly, the Pump Plunger Dynamic Seal and Reservoir Seal could be Silicone or SBR elastomer. The remaining o-rings have been determined to be a match for EPDM elastomer.

The solid residue from the reservoir filter was determined to be Silicone Grease and silicone brake fluid based on FTIR analysis. However, the FTIR spectral bands obtained on HPB servo valves corresponded to butadiene and phenyl groups in SBR. As a result, the used brake fluid that these servo valves were exposed to was filtered and the residue was analyzed. SEM imaging indicated the presence of threaded structures in addition to spherical agglomerates indicating the presence of polymer or elastomer compounds. XRD results indicated the presence of 1,4-Diphenyl-1,3-butadiene which is the monomer repeating unit of SBR elastomer. Therefore, the overall conclusion is that the root cause of deposit buildup is due to formation of a thin Styrene-Butadiene (SBR) elastomer residue on the servo valves.

Teardown and inspection of test hardware components for wear indicated light scuffing wear was evident between the pumping elements plungers and plunger barrels, and distress of the corresponding plunger elastomeric seals, with the unit that had undergone testing with the MIL-PRF-46176 brake fluid. The pumping elements that operated with DOT 3 brake fluid revealed light polishing and very little seal distress. Laboratory bench wear test results, (BOCLE and HFRR), also directionally indicated the MIL-PRF-46176 fluid was more severe in terms of wear. The reduced lubricity of the MIL-PRF-46176 silicone brake fluid and the fluids' sub-par compatibility with certain elastomers likely lead to the increased wear within the test rig and caused the deposit buildup observed in the reservoir and servo valve filters.

FOREWORD/ACKNOWLEDGMENTS

The U.S. Army TARDEC Fuel and Lubricants Research Facility (TFLRF) located at Southwest Research Institute (SwRI), San Antonio, Texas, performed this work during the period September 2014 through January 2016 under Contract No. W56HZV-09-C-0100. The U.S. Army Tank Automotive RD&E Center, Force Projection Technologies, Warren, Michigan administered the project. Mr. Eric Sattler (RDTA-SIE-ES-FPT) served as the TARDEC contracting officer's technical representative and Mr. Zackery Schroeder served as the project technical monitor.

The authors would like to acknowledge the contribution of the TFLRF technical and administrative support staff.

TABLE OF CONTENTS

<u>Section</u>	<u>Page</u>
EXECUTIVE SUMMARY	vi
FOREWORD/ACKNOWLEDGMENTS.....	viii
LIST OF FIGURES	x
LIST OF TABLES	xii
ACRONYMS AND ABBREVIATIONS	xiii
1.0 INTRODUCTION AND OBJECTIVE	1
2.0 ELASTOMER SEAL – BRAKE FLUID COMPATIBILITY STUDIES.....	1
2.1 STATIC AND DYNAMIC ELASTOMER TESTS	1
2.2 TECHNICAL BACKGROUND OF DYNAMIC ELASTOMER SEAL TESTER.....	2
2.3 TEST RIG: PRINCIPLE COMPONENT AND CONSTRUCTION.....	3
2.4 RECIPROCATING MOTION AND OPERATING LOAD	4
2.5 TEST RIG OPERATION, FAILURE CRITERION AND SWITCH LOADING.....	5
2.6 TESTING: MATERIALS AND MATRIX	5
2.7 RESULTS AND ANALYSIS.....	6
3.0 PHYSICAL AND CHEMICAL CHARACTERIZATION STUDIES.....	14
3.1 GC-MS ANALYSIS OF USED STATIC SOAK TEST BRAKE FLUIDS	14
3.2 PREDICTING IDENTITY OF ELASTOMER SEALS USING FTIR	14
3.3 ANALYSIS OF HSF FLUIDS AND SOLID RESIDUE FROM RESERVOIR FILTER	17
3.4 USED HSF BRAKE FLUID ANALYSIS	22
4.0 HYDRAULIC POWER BRAKE UNIT HARDWARE ANALYSIS.....	26
4.1 HYDRAULIC POWER BRAKE PUMPING ELEMENT ANALYSIS.....	26
4.2 HYDRAULIC POWER BRAKE SERVO VALVE REMOVAL.....	40
5.0 BRAKE FLUID PROPERTIES AND LUBRICITY.....	43
6.0 CONCLUSIONS.....	44
7.0 REFERENCES	46
APPENDIX A. ELASTOMER PROPERTY MEASUREMENTS.....	A-1
APPENDIX B. GC-MS SPECTRA	B-1

LIST OF FIGURES

<u>Figure</u>	<u>Page</u>
Figure 1. SwRI Dynamic Seal Tester	2
Figure 2. Principle Component of the Test Rig (Test Block)	3
Figure 3. Insulated Test Block Supported on a Rigid Aluminum Frame	4
Figure 4. Soak Test Results – Elastomer Thickness Change at Room Temperature versus 40 °C	10
Figure 5. Soak Test Results – Elastomer Hardness Change at Room Temperature versus 40 °C	11
Figure 6. Soak Test Results – Elastomer Volume Change at Room Temperature versus 40 °C	12
Figure 7. Soak Test Results – Tensile Strength Comparison at Room Temperature	13
Figure 8. Soak Test Results – Tensile Strength Comparison at 40 °C	13
Figure 9. FTIR for Pump Plunger Dynamic Seal and Reservoir Seal	15
Figure 10. FTIR for Pump Parking Brake Supply (Valve Body Seal) and Relay Valve Seal	15
Figure 11. FTIR for Bushing Lower and Middle Seal	16
Figure 12. FTIR for Parking Brake Supply (Valve Stem Seal) and Pump Barrel Seal	16
Figure 13. FTIR for Parking Accumulator, Busing Upper and Pump Upper Seal	17
Figure 14. Overlaid FTIR Traces for New and Used Silicon Brake Fluids and Filter Residue	18
Figure 15. FTIR Region of Interest for Particulate Residue	18
Figure 16. MIL-PRF-46176 Brake Fluid Filter Deposit	19
Figure 17. Filter Debris Elemental Analysis	20
Figure 18. FTIR Spectra of Four Servo Valve Filters and Fresh Silicone Brake Fluid	21
Figure 19. Filtered Residue from Used HSF	22
Figure 20. Elemental Analysis of Filtered Residue from used HSF	23
Figure 21. SEM Images of the Filtered Residue	25
Figure 22. XRD Results of the Filtered Residue	26
Figure 23. Disassembled Hydraulic Power Brake Pumping Element	27
Figure 24. Hydraulic Power Brake Pumping Plunger Detail	27
Figure 25. LF Plunger Overview from HSF Testing	28
Figure 26. LF Plunger Overview from Baseline Testing	29
Figure 27. Detail of the HSF LF Plunger Pumping Section Polishing and Wear	29
Figure 28. Detail of the Baseline LF Plunger Pumping Section Polishing and Wear	30
Figure 29. Close up of the HSF LF Plunger Follower Section Polishing and Wear	30
Figure 30. Close up of the Baseline LF Plunger Follower Section Polishing and Wear	31
Figure 31. Sectioned HSF LF Barrel with Bore Wear from Follower	32
Figure 32. Sectioned Baseline LF Barrel with Bore Wear from Follower	32
Figure 33. Elastomer on LF Plunger from HSF Testing	33
Figure 34. Elastomer on LF Plunger from Baseline Testing	33
Figure 35. LR Plunger Overview from HSF Testing	34
Figure 36. LR Plunger Overview from Baseline Testing	35
Figure 37. Detail of the HSF LR Plunger Pumping Section Polishing and Wear	35
Figure 38. Detail of the Baseline LR Plunger Pumping Section Polishing and Wear	36
Figure 39. Close up of the HSF LR Plunger Follower Section Polishing and Wear	36
Figure 40. Close up of the Baseline LR Plunger Follower Section Polishing and Wear	37
Figure 41. Sectioned HSF LR Barrel with Bore Wear from Follower	38

LIST OF FIGURES (CONT'D)

<u>Figure</u>	<u>Page</u>
Figure 42. Sectioned Baseline LR Barrel with Bore Wear from Follower.....	38
Figure 43. Elastomer on LR Plunger from HSF Testing	39
Figure 44. Elastomer on LR Plunger from Baseline Testing.....	39
Figure 45. Valves sliced from the main block using a band saw.....	40
Figure 46. Parallel cuts were made along each row, with valves numbered as indicated	41
Figure 47. Cuts were then made perpendicular to the row cuts to isolate each valve and filter unit.....	41
Figure 48. Small cuts were made on 3 sides as indicated.....	42
Figure 49. A hammer and chisel was then used to crack open the case and the valve and filter were then removed	42

LIST OF TABLES

<u>Table</u>	<u>Page</u>
Table 1. Static Soak and Dynamic Seal Test Matrix	6
Table 2. Summary of Results from Dynamic Seal Tests	6
Table 3. HBP Elastomer Identification using FTIR.....	14
Table 4. Elemental Analysis of Deposit.....	20
Table 5. Relative Elemental Concentration of Residue from used HSF.....	23
Table 6. Brake Fluid Property Analysis.....	43
Table 7. Bench Wear Test Results for Brake Fluids.....	44

ACRONYMS AND ABBREVIATIONS

° C	degrees Centigrade
ASTM	ASTM International
BOCLE	Ball On Cylinder Lubricity Evaluator
CI	corrosion inhibitor
cm	Centimeter
CRC	Coordinating Research Council
cSt	Centistokes
DOT	Department of Transportation
ft	Foot
EPDM	Ethylene Propylene Diene Monomer
HFRR	High Frequency Reciprocating Rig
HPB	Hydraulic Power Brake
HSF	Hydraulic Silicone Fluid
hr	Hour
in	Inch
L	Liter
lb	Pound
lb _f	pound (force)
lb _m	pound (mass)
m	Meter
mg	Milligram
mm	Millimeter
OEM	Original Equipment Manufacturer
ppm	parts per million
psi	pounds per square inch
psiA	pounds per square inch, absolute
psiG	pounds per square inch, gauge
SAE	Society of Automotive Engineers
SBR	Styrene Butadiene Rubber
SwRI [®]	Southwest Research Institute [®]
SOW	Scope of Work
TACOM	Tank Automotive and Armaments Command
TARDEC	Tank Automotive RD&E Center
TFLRF	TARDEC Fuel and Lubricants Research Facility
WD	work directive
WEDM	Wire Electrostatic Discharge Machining

1.0 INTRODUCTION AND OBJECTIVE

The Army converted its tactical vehicles to silicone brake fluid (Hydraulic Silicone Fluid, HSF) in the early 1980's to address corrosion problems with the previous glycol based fluid. Fielded Army tactical vehicles do not currently run advanced brake systems such as anti-lock brakes and stability control. The current military brake fluid, MIL-PRF-46176 Silicone Brake Fluid (HSF), has not been applied in the use of advanced brake systems commercially. The compatibility of Army HSF with heavy duty anti-lock brake systems needs to be determined. Fluids to be investigated include: commercially available SAE J1703, silicone brake fluid meeting MIL-PRF-46176 (both dyed and undyed), and MIL-PRF-46176 base stock.

There have been reports of possible high temperature degradation of the brake fluid leading to deposits and filter plugging, and filter collapse. An anti-lock brake testing system which integrates the Meritor-WABCO Hydraulic Pressure Brake (HPB) test system was established in Fiscal Year 2013 (FY13) for testing purposes. Testing in FY13, reported in TFLRF Interim Report No. 445 [1], showed deposit build-up in the system reservoir that caused testing to halt when testing MIL-PRF-46176. Deposits were not present in SAE J1703 testing for the same number of test cycles. The objective of this program was to investigate and determine the root cause of the particle build-up. System hardware from prior testing was inspected, and deposits and fluids analyzed. Lubricity tests and dynamic seal tests were conducted using various brake fluids.

2.0 ELASTOMER SEAL – BRAKE FLUID COMPATIBILITY STUDIES

2.1 STATIC AND DYNAMIC ELASTOMER TESTS

The objective was to compare the compatibility of elastomer seals in new Silicone Brake Fluid (HSF) against SAE J1703 as the baseline fluid using static and dynamic seal tests. The difference in physical properties of the elastomer o-rings, such as, weight, thickness, hardness, volume swell and tensile strength, from pre-test and post-test conditions, between HSF and baseline fluid, compared the impact of brake fluids on the elastomer material. In static soak tests, the

elastomer properties was compared for soak tests conducted at room temperature and at 40 °C. However, in dynamic seal tests, the impact of brake fluid was assessed and compared based on the combined action of reciprocating motion and at 40 °C operating temperature. The static soak and dynamic seal test collectively generated three sets of data, namely, at room temperature under static conditions, at 40 °C under static conditions, and at 40 °C under dynamic conditions. This data was used to address the impact of brake fluids on elastomer materials.

2.2 TECHNICAL BACKGROUND OF DYNAMIC ELASTOMER SEAL TESTER

A detailed description of the dynamic seal test rig construction and operation was presented in TFLRF Report No. 371 [2]. Turbojet engine control systems employ sealing surfaces that move or slide over an elastomer sealing material. These seals are generally referred to as dynamic seals, and the usual configuration is an o-ring. SwRI designed and built a laboratory bench-top apparatus, which is shown in Figure 1. This apparatus, called the dynamic seal test rig, was used for the evaluation of elastomeric o-rings exposed to various fluids or fuels, on a reciprocating shaft, under dynamic conditions. The test rig was designed to simulate temperatures ranging from 15 °F to 300 °F. The dynamic tests were used to study the effect of brake fluids on properties and performance of elastomeric materials.



Figure 1. SwRI Dynamic Seal Tester

2.3 TEST RIG: PRINCIPLE COMPONENT AND CONSTRUCTION

The dynamic seal test rig simulated sealing conditions normally employed for sealing a shaft that reciprocates in its axial direction. Figure 2 shows a cross-section drawing of the principal component of the test rig. A stainless steel shaft with test o-rings, machined to highly precise dimensions (± 0.005 inch), was reciprocated in a heated aluminum block containing a precision bore. A small cavity at the end of each aluminum block, formed within the end caps, collected fuel that leaks past the o-ring under test. The “primary seal” was the seal under test and the function of the “secondary seal” was to prevent fuel from leaking through the fuel collection cavity. The end cap was also sealed against the body via an o-ring seal (AS-568116). Two elastomeric o-rings (size AS-568-012) were installed in the shaft. A 600-W band heater controlled the fuel temperature within the central cavity to the desired test temperature. The fuel temperature should not exceed 300 °F. Type T thermocouples are located in the test block to measure the actual temperature of each o-ring. The cavity temperature was controlled by measurements from only one of the thermocouples, but either one can be selected. The measured temperature was always monitored and displayed from both the o-ring locations.

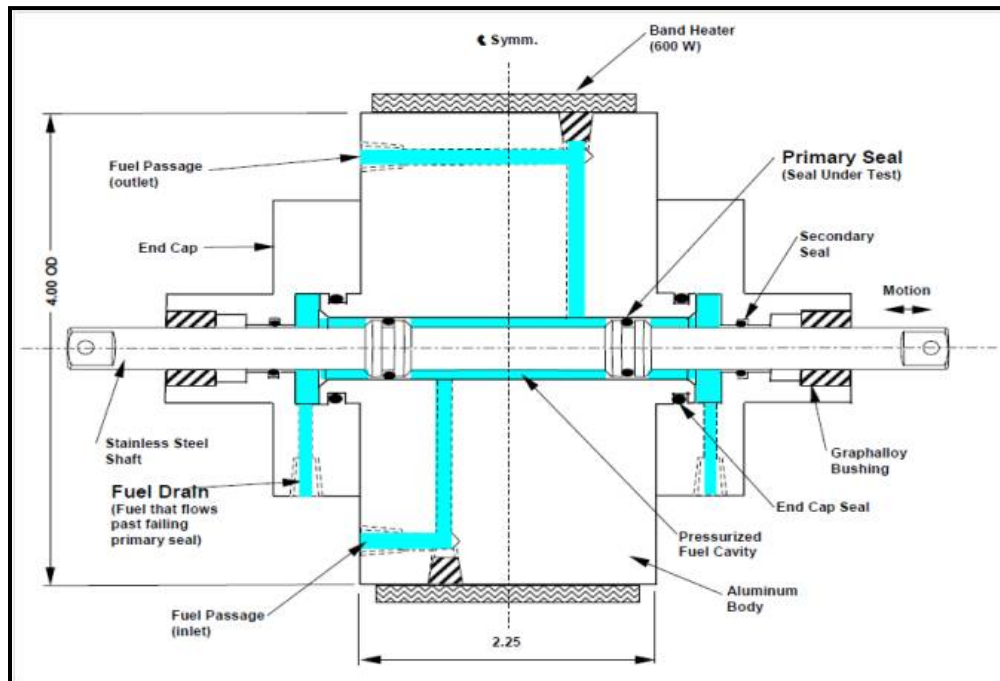


Figure 2. Principle Component of the Test Rig (Test Block)

2.4 RECIPROCATING MOTION AND OPERATING LOAD

The heated insulated block and shaft were supported on a rigid aluminum frame structure as shown in Figure 3. The force needed to move the shaft was directed in the shaft's axial direction and precisely collinear on the axial centerline of the shaft. This was accomplished by a cross-head assembly incorporating two linear bearings. The force was supplied by a 12-rpm, $\frac{3}{4}$ -horsepower gear-motor connected to a bell-crank mechanism. The shaft horizontal displacement was set to $\pm 3/16$ ". The stroke could be slightly adjusted by setting the radial distance of the bell-crank pin. The stroke was not more than $\pm 1/4$ " because the shaft must keep its stroke within the allowable length.

The total distance traversed by the reciprocating shaft in one direction was 0.375". The angular velocity (ω), computed using rpm, is $(2\pi/5)$ rad/s. The conversion of bell-crank rotary motion to reciprocating motion yielded a sinusoidal velocity distribution. The corresponding force exerted on the o-rings was time dependent and was a function of the product of angular velocity and time (ωt). However, dynamics of motion was not the focus of this research. The time taken for a single stroke in one direction was 2.5 s, over a distance of 0.375". For a $\frac{3}{4}$ -horsepower motor, the total load imparted to the o-rings due to reciprocating motion, per stroke in a single direction, was 146.79 KN.

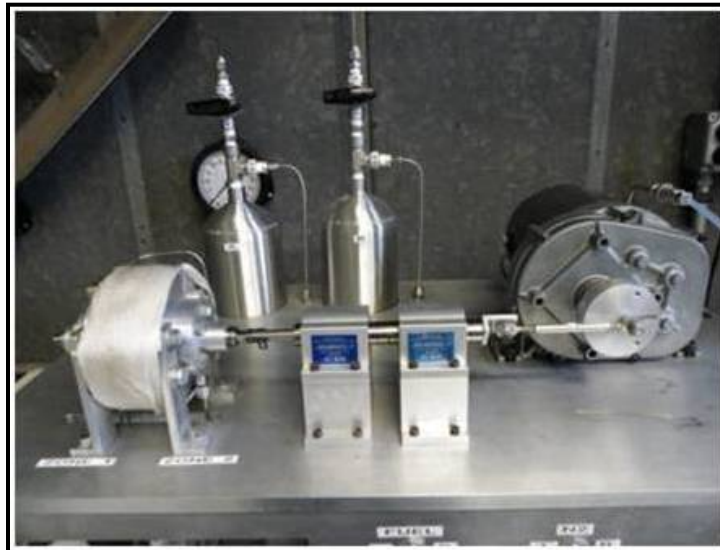


Figure 3. Insulated Test Block Supported on a Rigid Aluminum Frame

2.5 TEST RIG OPERATION, FAILURE CRITERION AND SWITCH LOADING

Two AS568-O12 o-rings of the same material were mounted on a reciprocating shaft as shown in Figure 2. The thickness, hardness, and volume of the o-rings were measured prior to installation. The fluid sample under investigation was filled in either of the two reservoirs. The reservoir was pressurized to about 80 psig with Nitrogen. The 600-W heater was set to control the fluid temperature during the test. The motor set the reciprocating shaft in motion prior to turning on the heater. The thermocouples were positioned closer to the internal wall of the test block (shown in Figure 2). Fluid leaking past the seals under test was captured in two 5-ml graduated cylinders located just below the heated block. A photoelectric sensor was incorporated to stop the test after a certain volume of leaked fluid was collected in either of these graduated cylinders. The failure criterion was defined as the time needed for the seal to fail and leak fluid from the test block into the graduated cylinders before 400 hours of test time. In dynamic seal tests the changes in elastomer properties and failure time provided an insight into seal performance with a variety of brake fluids. A unique feature of the test rig was its ability to switch fluids during a test run. The test can start with one particular fluid that was brought into contact with the o-ring seals and then switched to a second fluid with a different composition. This simulated a situation that occurs in the field where there are frequent changes of fluid composition on elastomers. Two reservoirs and associated valves in the test rig were used to accomplish the switch loading manually.

2.6 TESTING: MATERIALS AND MATRIX

The four elastomer seal materials used for the study were: Ethylene Propylene Diene Monomer (EPDM), Silicone, Neoprene, Styrene Butadiene Rubber (SBR). The two fluids used for static soak and dynamic seal tests were: HSF and SAE J1703 base fluid. For static soak tests, three o-rings of size AS-568-O17, per elastomer type, per fluid were used for testing. This size was compatible for tensile strength measurements in addition to thickness, hardness and volume swell properties. However, the dynamic seal tester was only designed to accommodate smaller o-rings of size AS-568-O12, and therefore tensile strength property was not determined for the elastomers used in dynamic seal tests. In lieu of tensile strength, pre-test and post-test weight measurements were made for elastomers in dynamic seal tests, as a way to identify dissolution of elastomer constituents into the fluid. Two o-rings of size AS-568-O12 per elastomer type, per fluid, were

used. The soak tests were conducted at ambient temperature and at 40 °C. Table 1 provides a summary of the test matrix. The property measurement methods are described in APPENDIX A.

Table 1. Static Soak and Dynamic Seal Test Matrix

Fluid	Elastomer	Property Measurements (Pre-test and Post-test)		
		Static Soak Test		Dynamic Seal Test
		Ambient Temperature	Test Temperature = 40 °C	Test Temperature = 40 °C
HSF	EPDM	Thickness, Hardness, Volume Swell, and Tensile Strength, Three o-rings (AS-568-O17)	Thickness, Hardness, Volume Swell, and Tensile Strength, Three o-rings (AS-568-O17)	Weight, Thickness, Hardness, and Volume Swell, Two o-rings (AS-568-O12)
	Neoprene			
	Silicone			
	SBR			
SAE J1703	EPDM	Thickness, Hardness, Volume Swell, and Tensile Strength, Three o-rings (AS-568-O17)	Thickness, Hardness, Volume Swell, and Tensile Strength, Three o-rings (AS-568-O17)	Weight, Thickness, Hardness, and Volume Swell, Two o-rings (AS-568-O12)
	Neoprene			
	Silicone			
	SBR			

2.7 RESULTS AND ANALYSIS

The summary of results for dynamic seal tests, in terms of percentage change in thickness, hardness, weight and volume change, is listed in Table 2.

Table 2. Summary of Results from Dynamic Seal Tests

Fluid: HSF; Left o-ring					
#	Material	ΔThickness (%)	ΔHardness (%)	ΔWeight (%)	ΔVolume (%)
1	EPDM (400 hrs)	0.61	2.10	0.38	2.69
2	Neoprene (400 hrs)	0.11	0.58	0.53	2.31
3	Silicone (398 hrs, 5mL)	-25.73	-39.63	12.29	36.23
4	SBR (400 hrs)	6.42	-9.08	8.34	12.60
Fluid: SAE J1703; Left o-ring					
#	Material	ΔThickness (%)	ΔHardness (%)	ΔWeight (%)	ΔVolume (%)
1	EPDM (400 hrs)	-5.31	-10.78	2.62	10.72
2	Neoprene (237.4 hrs, 2.5mL)	-2.87	-3.42	-0.15	5.08
3	Silicone (400 hrs)	-7.53	-1.33	4.53	8.29
4	SBR (400 hrs)	-0.87	-2.91	-0.87	4.44
Fluid: HSF; Right o-ring					
#	Material	ΔThickness (%)	ΔHardness (%)	ΔWeight (%)	ΔVolume (%)
1	EPDM (400 hrs)	-1.34	2.49	1.84	3.86
2	Neoprene (400 hrs)	-0.08	-0.30	1.74	2.56
3	Silicone (398 hrs, 2mL)	-37.94	-48.75	-9.74	4.09
4	SBR (400 hrs)	6.58	-9.79	7.65	13.03
Fluid: SAE J1703; Right o-ring					
#	Material	ΔThickness (%)	ΔHardness (%)	ΔWeight (%)	ΔVolume (%)
1	EPDM (400 hrs)	-4.68	-7.90	2.69	4.78
2	Neoprene (237.4 hrs, 0.5 mL)	-2.71	-5.45	1.64	10.67
3	Silicone (400 hrs)	-7.42	-10.80	4.50	7.73
4	SBR (400 hrs)	-0.02	-5.47	-0.38	2.32

It should be noted that the dynamic seal test results were obtained for a pair of o-rings and therefore statistics have not been computed. The following conclusions can be drawn from the dynamic seal test results:

- a. EPDM, Neoprene, and SBR completed the total test time of 400 hours with HSF, while Silicone elastomer failed at 398 hours. For SAE J1703 fluid, EPDM, Silicone and SBR completed the entire test, while, Neoprene failed the test 237.4 hours. It can be concluded that in terms of performance, compared to the baseline brake fluid, that the silicone brake fluid improves the performance of Neoprene elastomer and deteriorates the performance of silicone elastomer.
- b. For EPDM elastomer, the thickness decreases for both brake fluids. The increase in thickness, 0.61% for HSF fluid for left o-ring, can be considered insignificant for all practical purposes. It was inferred that the overall hardness of EPDM elastomer increases with the use of a silicone brake fluid compared to the baseline SAE J1703 fluid. The increase in elastomer weight and volume swell was lower for EPDM, in silicone brake fluid compared to the baseline fluid.
- c. For Neoprene, there was negligible change in thickness and hardness of the elastomer in silicone brake fluid compared to reduction in thickness in the baseline brake fluid. The overall tendency of the neoprene elastomer ranges from no weight change to at least some increase in weight, for both silicone brake fluid and the baseline brake fluid. The increase in elastomer volume swell was lower for Neoprene, in silicone brake fluid compared to the baseline fluid. This is worth mentioning due to the fact that increased volume swell resulting in abrasion could have been one of the factors in causing Neoprene to fail with the baseline fluid.
- d. In the case of Silicone elastomer, the decrease in thickness and hardness was much higher for silicone brake fluid compared to the decrease in thickness and hardness in baseline brake fluid. There was no meaningful interpretation gained from weight and volume change since the elastomer failed during dynamic test with silicone brake fluid.

- e. For SBR elastomer, the thickness increased in silicone brake fluid, whereas there was negligible thickness change in baseline brake fluid. The hardness decreased with both brake fluids, where the silicone brake fluid resulted in higher percentage decrease in hardness compared to the baseline brake fluid.
- f. The baseline brake fluid did not result in any weight change in the SBR elastomer, while there was a significant weight gain with silicone brake fluid. The volume swell was much higher with silicone brake fluid compared to the baseline brake fluid.

The static soak test results, in terms of percentage thickness, hardness, and volume change, along with tensile strength measurement comparison, are shown from Figure 4 to Figure 8. The following conclusions can be drawn from the static soak test results:

- a. At a given temperature, for thickness changes, Neoprene, Silicone and SBR elastomers exhibit the same trend, in that the silicone brake fluid did not reduce the thickness as much as the baseline SAE J1703 brake fluid. However, for EPDM the thickness changes are similar for both fluids at ambient temperature and for 40 °C, silicone brake fluid tended to reduce EPDM elastomer thickness compared to the baseline brake fluid.
- b. For hardness changes, for all the elastomers, at both ambient temperature and at 40 °C, silicone brake fluid reduced the hardness of all elastomers compared to baseline fluid.
- c. For volume swell measurements both at ambient temperature and 40 °C, all elastomers exhibited similar trends with both silicone brake fluid and baseline fluid. Neoprene and Silicone elastomers have slight volume swell with SAE J1703 fluid, while there is a significant volume swell for the same elastomers with silicone brake fluid.
- d. For SBR elastomer, there was a slight volume shrinkage with baseline brake fluid, and a significant volume swell was measured with silicone brake fluid, at both temperatures. For EPDM elastomer, there was slight volume shrinkage with the baseline brake fluid, at both temperatures.
- e. With the silicone brake fluid, EPDM showed both volume swell for some samples and volume shrinkage for others, leading the results to be inconclusive at ambient

temperature, whereas at 40 °C, EPDM samples showed volume shrinkage with silicone brake fluid.

- f. At ambient temperature, the tensile strength for EPDM elastomer was in the same ballpark for both brake fluids. The tensile strengths of Neoprene and SBR had overlapping ranges for both fluids and the comparison remains inconclusive. For Silicone elastomer, the silicone brake fluid decreased the tensile strength, at room temperature.
- g. At 40 °C, the tensile strengths of EPDM, Silicone and SBR decreased with silicone brake fluid relative to the SAE J1703 baseline brake fluid. For silicone elastomer, there was significant overlap between ranges and the results remain inconclusive.

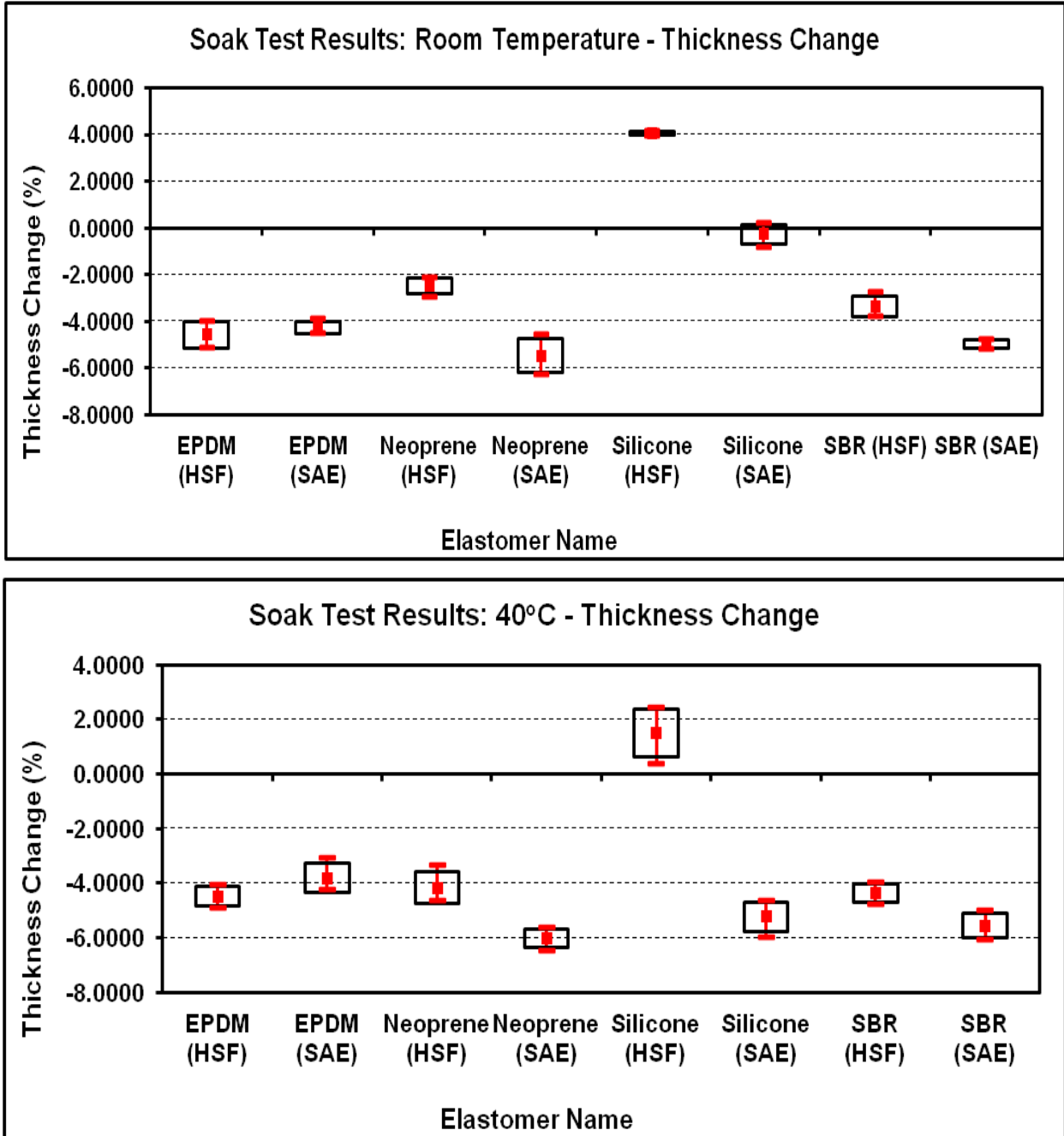


Figure 4. Soak Test Results – Elastomer Thickness Change at Room Temperature versus 40 °C

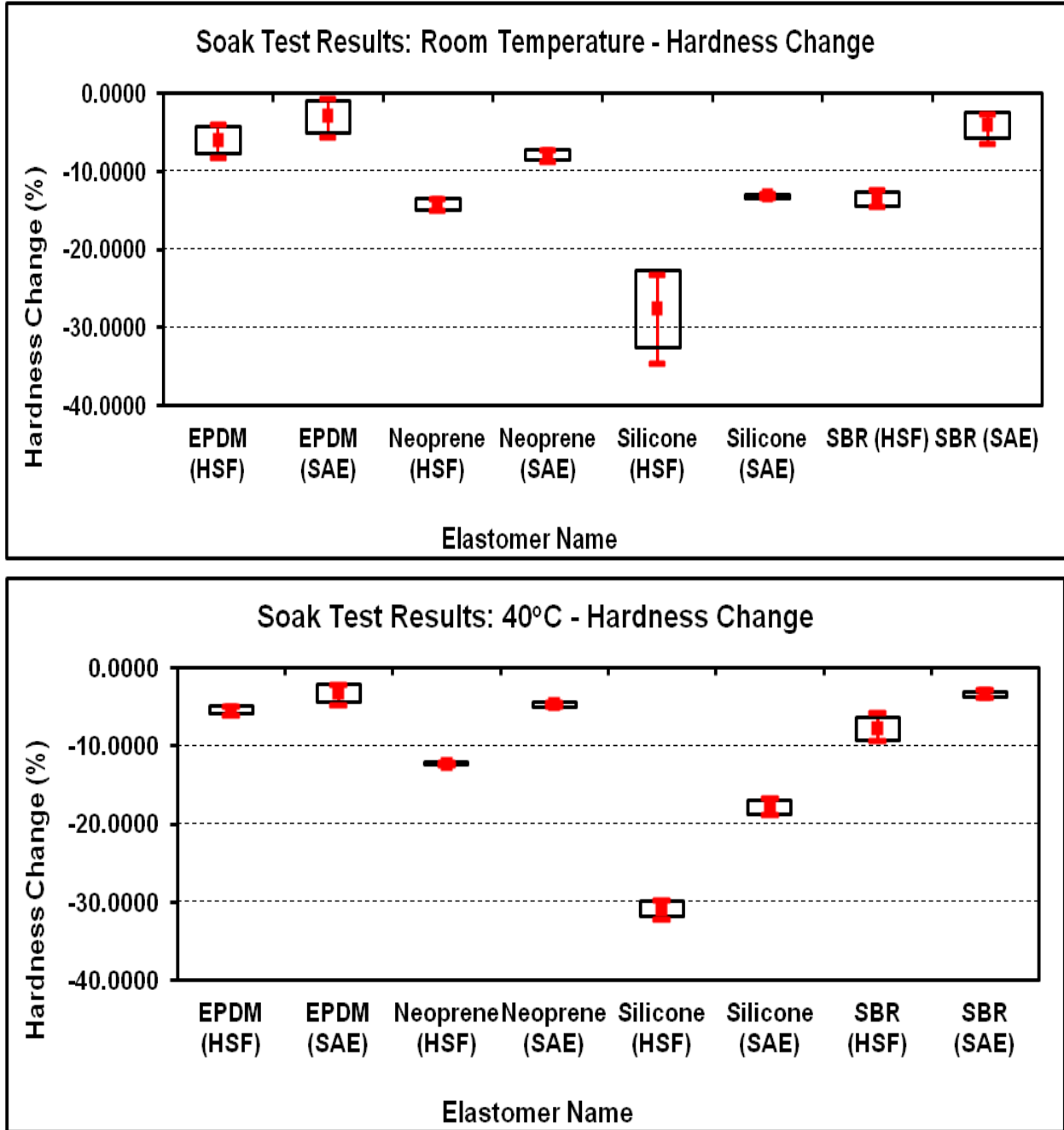


Figure 5. Soak Test Results – Elastomer Hardness Change at Room Temperature versus 40 °C

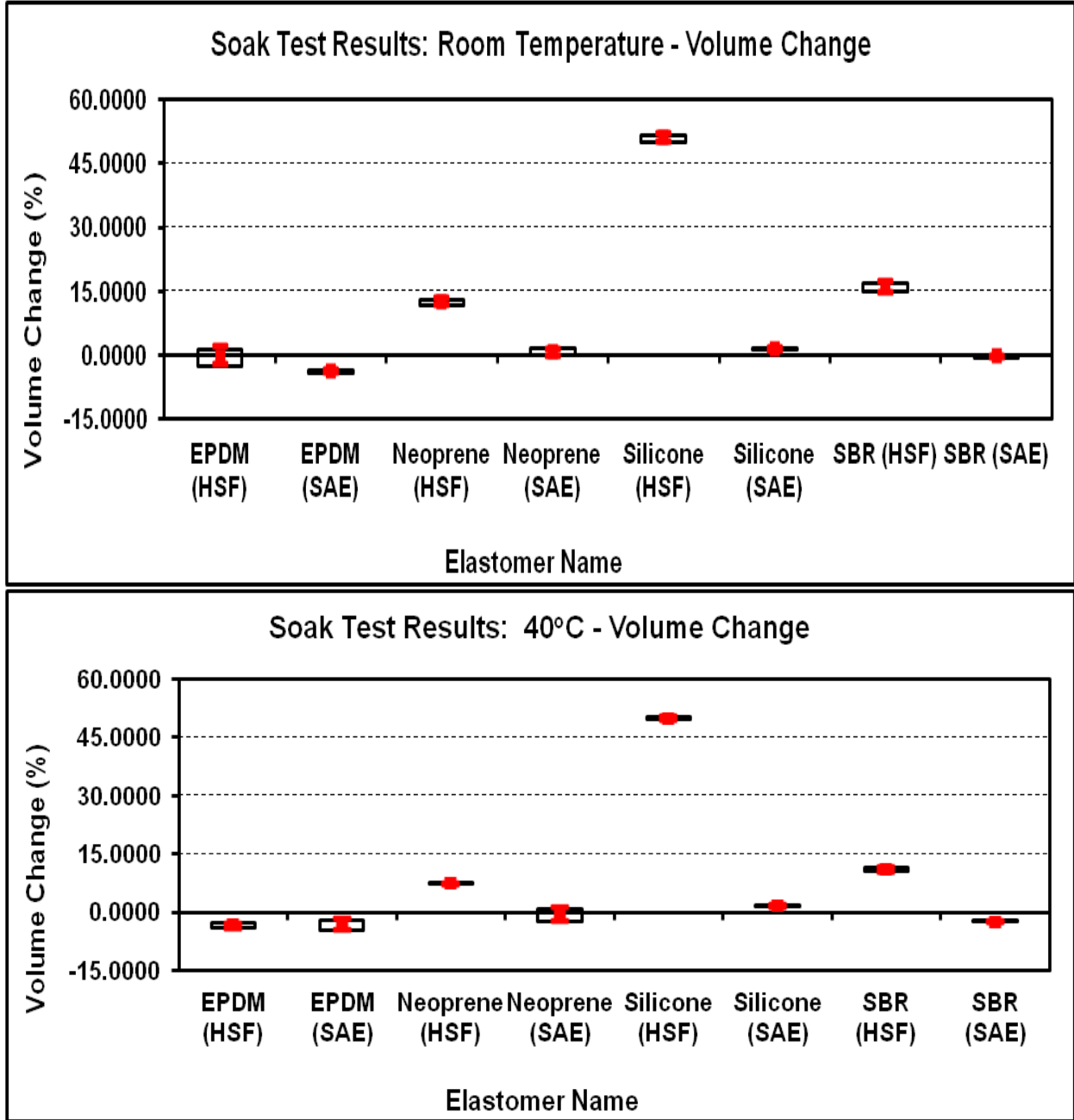


Figure 6. Soak Test Results – Elastomer Volume Change at Room Temperature versus 40 °C

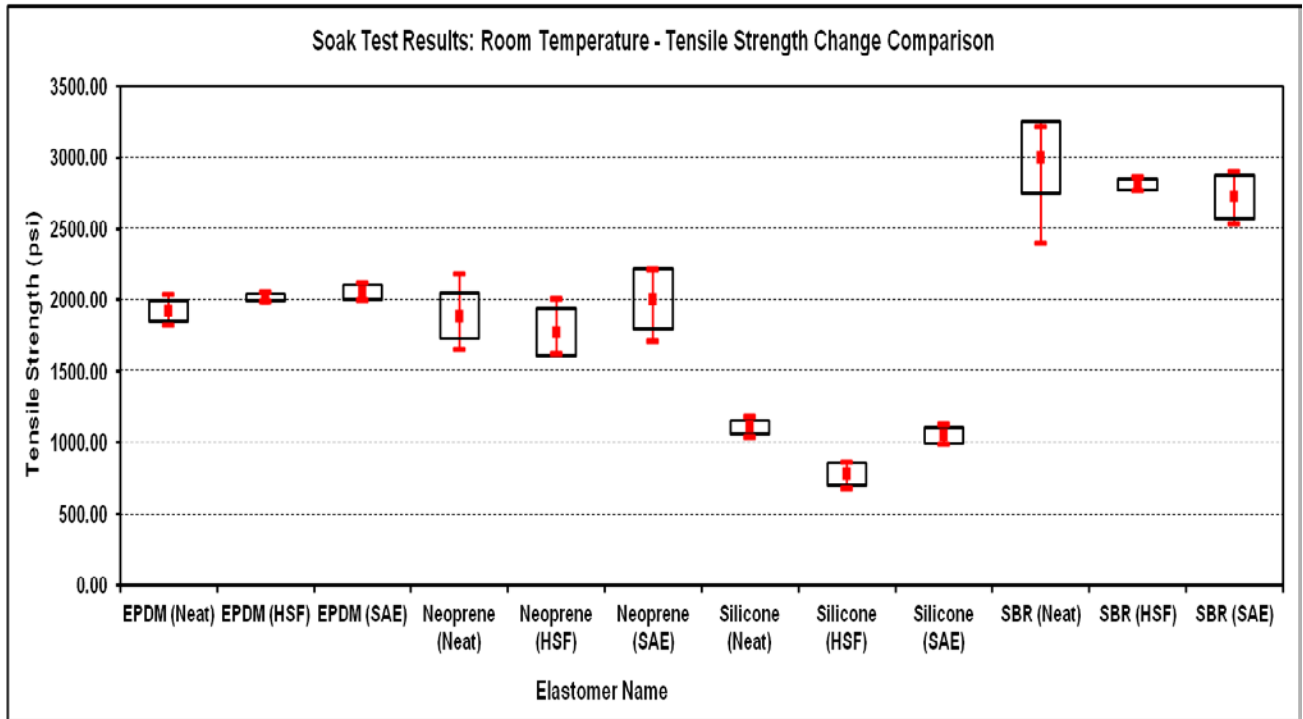


Figure 7. Soak Test Results – Tensile Strength Comparison at Room Temperature

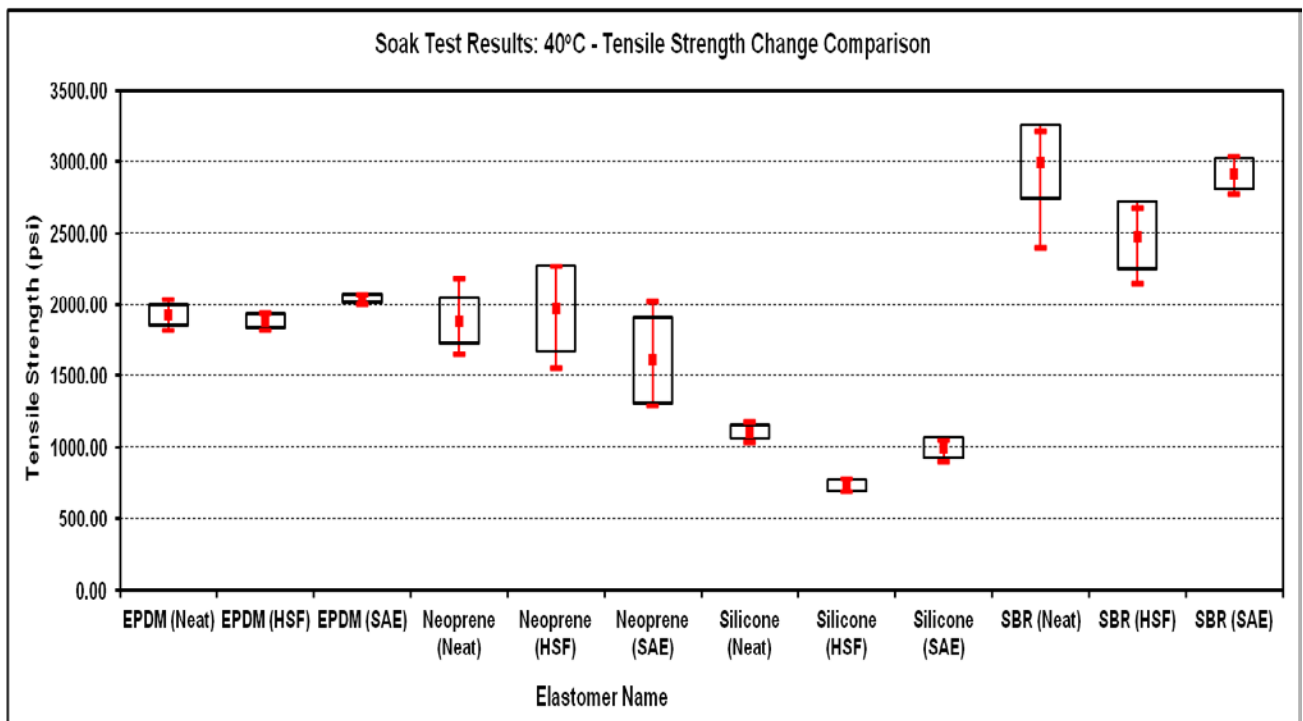


Figure 8. Soak Test Results – Tensile Strength Comparison at 40 °C

3.0 PHYSICAL AND CHEMICAL CHARACTERIZATION STUDIES

3.1 GC-MS ANALYSIS OF USED STATIC SOAK TEST BRAKE FLUIDS

The used brake fluids from static soak tests were analyzed using GC-MS to determine if any elastomer had leached into the brake fluid. GC-MS for neat silicone brake fluid and SAE J1703 baseline fluid was obtained and compared with the GC-MS data from the used brake fluids from static soak tests to identify if any elastomer peaks were present. A total of sixteen comparisons were made for four elastomers soaked in two brake fluids at two temperatures. It was inferred that no elastomers were present in the used static soak test fluids. This indicated that the elastomer did not leach into the brake fluids. The GC-MS spectra, for neat brake fluids and the overlays are presented in APPENDIX B.

3.2 PREDICTING IDENTITY OF ELASTOMER SEALS USING FTIR

The eleven elastomer seals from various Hydraulic Pressure Brake (HPB) components were identified using FTIR as shown in Table 3.

Table 3. HBP Elastomer Identification using FTIR

#	Component Seal Name	Likely Elastomer Identity
1	Parking Brake Supply (Valve body seal) [o-ring] Relay Valve Seal [o-ring]	EPDM or SBR
2	Pump Plunger Dynamic Seal [Lip] Reservoir Seal [T-shaped Bushing]	Silicone Elastomer or SBR
3	Accumulator Seal [o-ring] Parking Brake Valve Bushing Upper Seal [o-ring] Pump Body Upper Seal [o-ring]	Poly(isoprene) rubber (EPDM)/Silica filled
4	Parking Brake Supply (Valve Stem Seal) [o-ring] Pump Barrel Seal [o-ring]	Poly(isoprene) rubber (EPDM) plus filler (possibly SiO ₂)
5	Parking Brake Valve Bushing Lower Seal [o-ring] Parking Brake Valve Bushing Middle Seal [o-ring]	Poly(isoprene) rubber (EPDM) plus filler (possibly SiO ₂)

The FTIR spectra for the HPB components are shown from Figure 9 to Figure 13. The identity of Parking Brake Supply and Relay Valve Seal remains unclear due to proprietary nature of filler combinations used in the elastomer; it could be either EPDM or SBR. Similarly, Pump Plunger Dynamic Seal and Reservoir Seal could be Silicone or SBR elastomer. The remaining o-rings were determined to be a match for EPDM elastomer. The fillers (either silica or SiO₂) are commonly used in the elastomer o-rings.

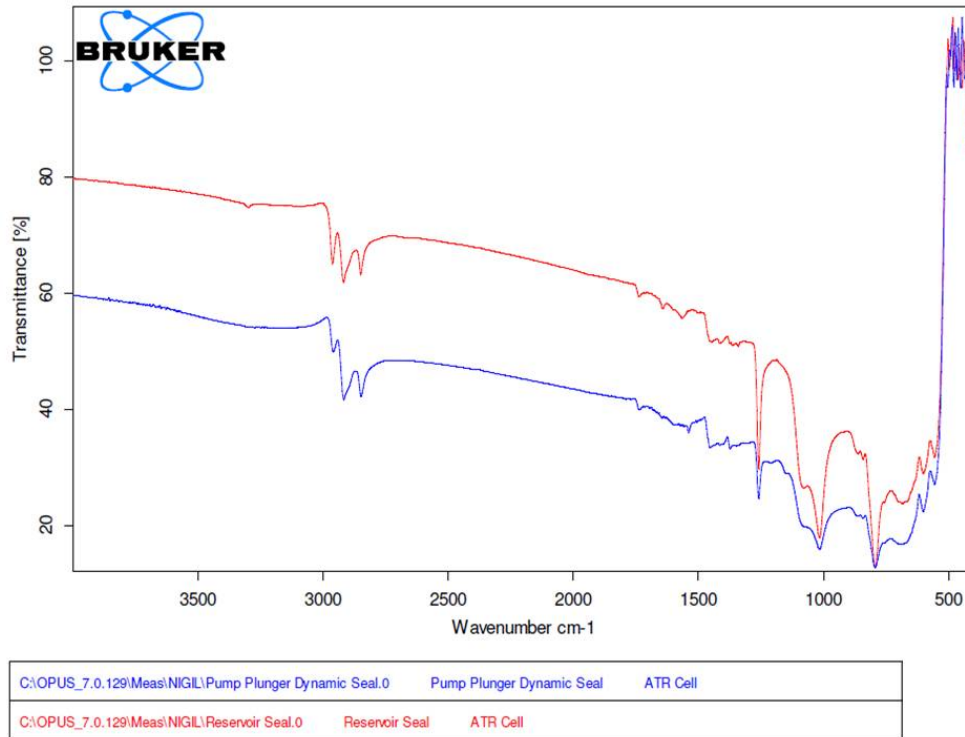


Figure 9. FTIR for Pump Plunger Dynamic Seal and Reservoir Seal

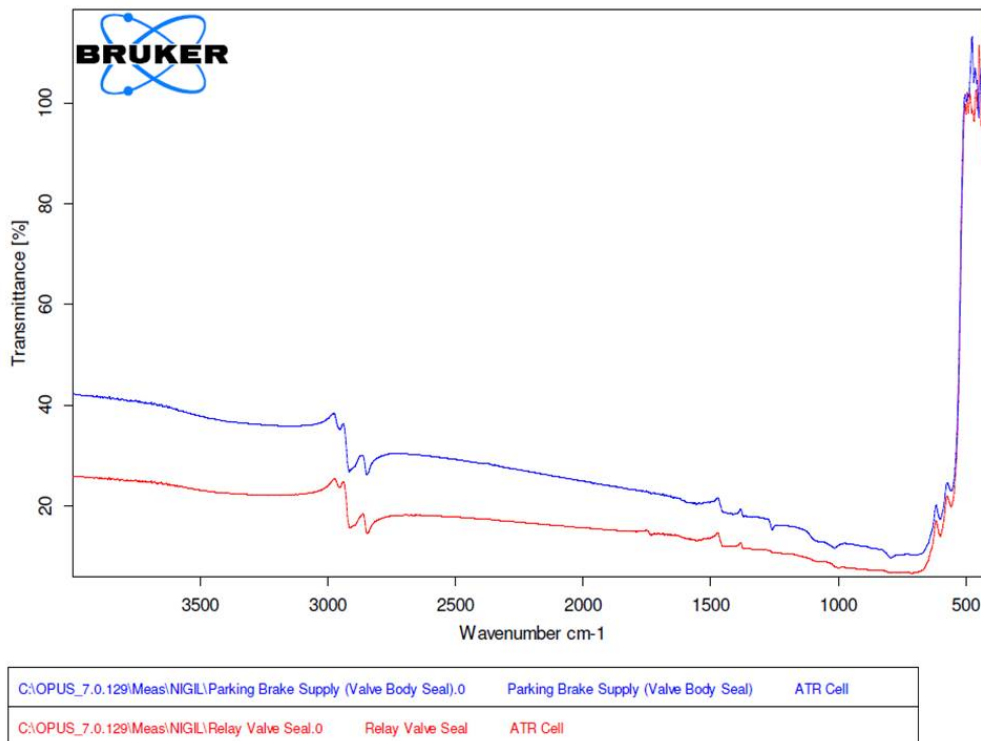


Figure 10. FTIR for Pump Parking Brake Supply (Valve Body Seal) and Relay Valve Seal

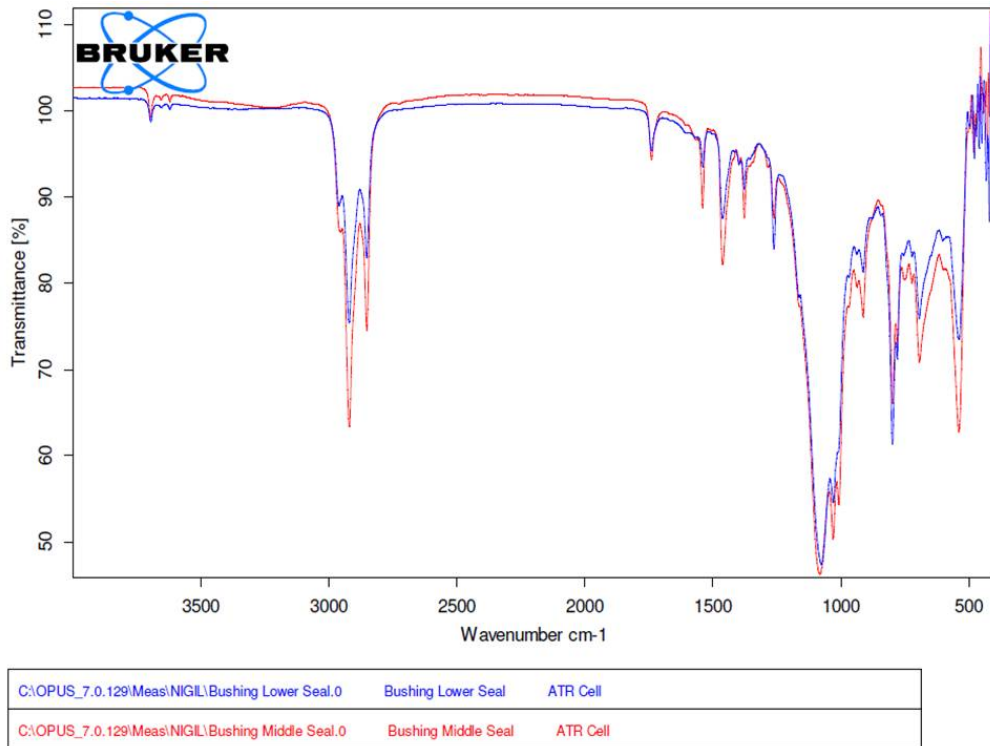


Figure 11. FTIR for Bushing Lower and Middle Seal

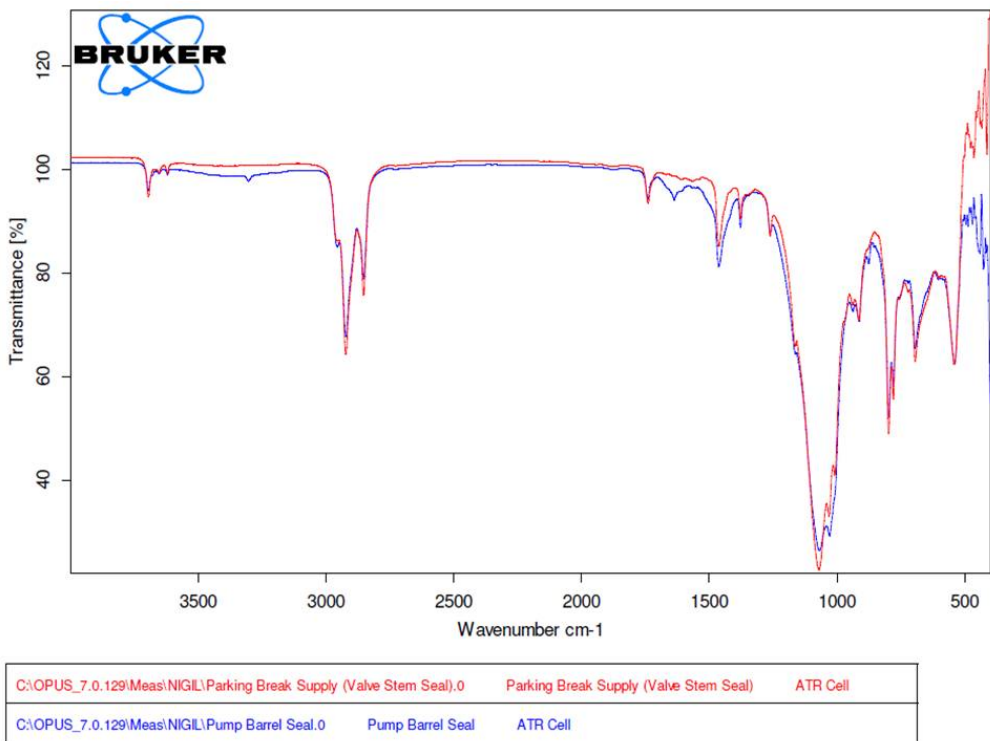


Figure 12. FTIR for Parking Brake Supply (Valve Stem Seal) and Pump Barrel Seal

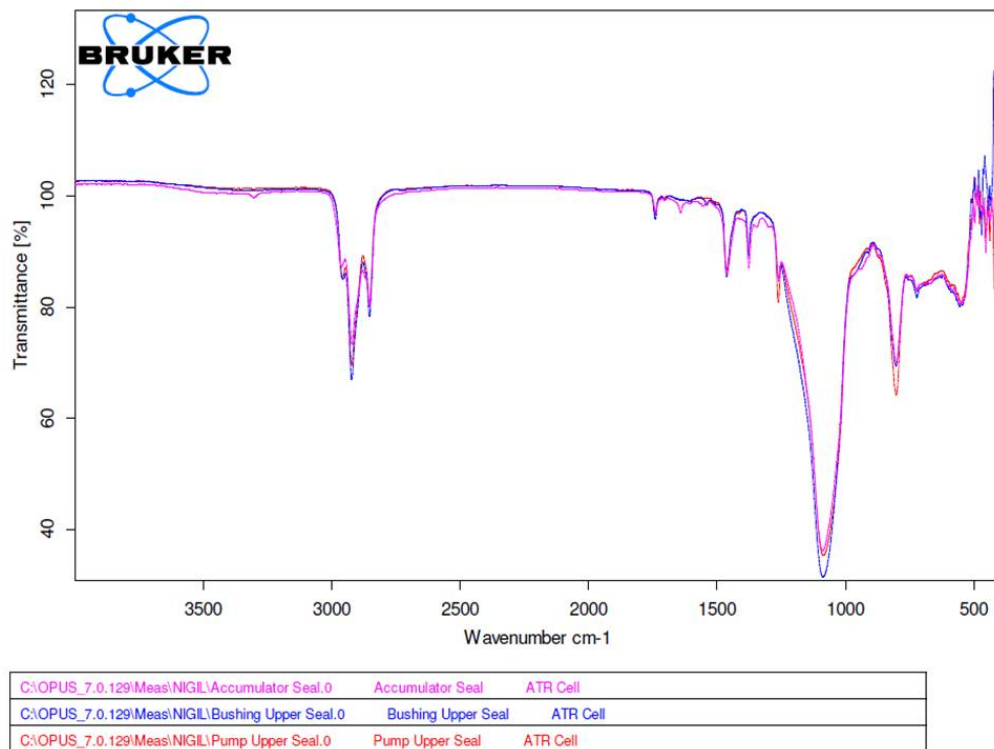


Figure 13. FTIR for Parking Accumulator, Busing Upper and Pump Upper Seal

3.3 ANALYSIS OF HSF FLUIDS AND SOLID RESIDUE FROM RESERVOIR FILTER

FTIR spectra were obtained for new silicone brake fluid (HSF), used silicone brake fluid (top and bottom fluid layers), and the solid residue recovered from a reservoir filter. Overlaying all the spectra, Figure 14 and Figure 15 (magnified), indicated the following spectral bands that were present in the residue and not in the silicone brake fluids (either used or new): 1593.63 cm^{-1} indicates C–C stretch in a ring signifying presence of aromatic compounds in the solid residue; 1562.09 cm^{-1} indicated compounds containing N–O asymmetric ring stretch signifying nitro compounds; 1399.14 cm^{-1} and 1370.75 cm^{-1} indicated compounds containing N=O bends signifying nitro compounds.

The above spectral bands likely points to the presence of Nitrile based compounds in the solid residue. However, FTIR spectra of elastomer seals from HBP components in Table 3, did not contain Nitrile based elastomers. Therefore, the spectral bands from FTIR spectra in Figure 14 and Figure 15, were not from Nitrile elastomers, rather could be an artifact of other constituents present in the fluid.

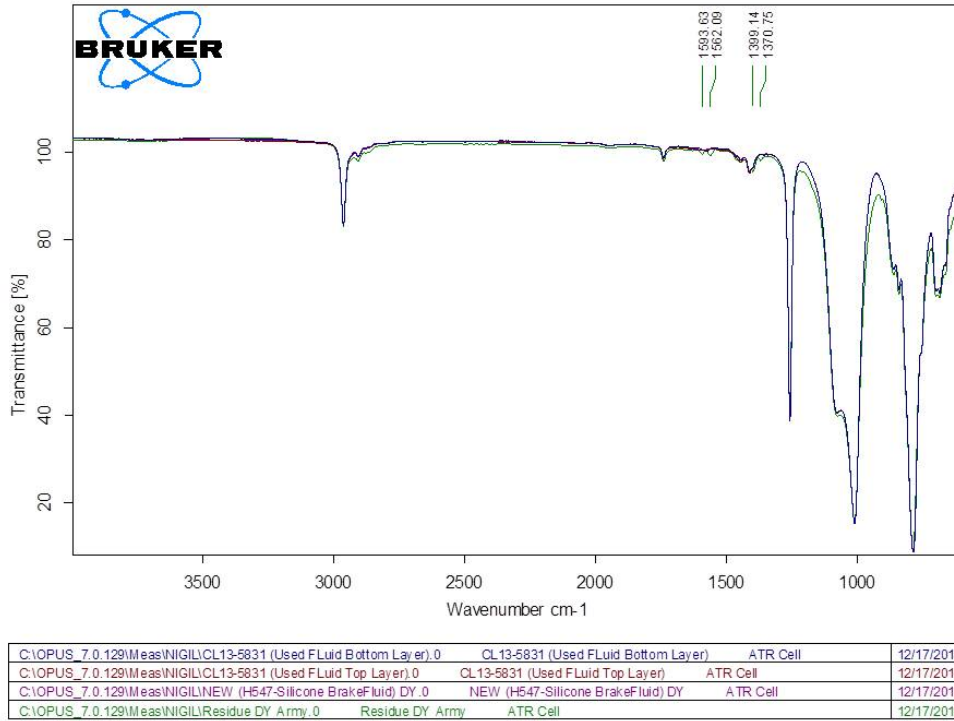


Figure 14. Overlaid FTIR Traces for New and Used Silicon Brake Fluids and Filter Residue

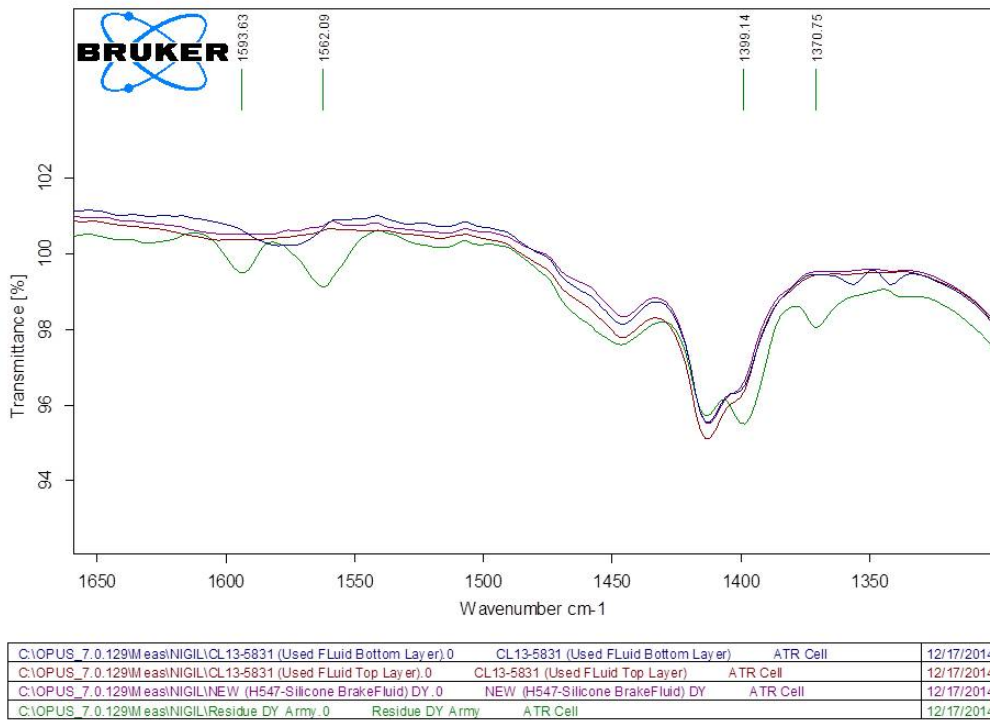


Figure 15. FTIR Region of Interest for Particulate Residue

Since the exact identity of the deposit from the HPB filter could not be determined using FTIR technique the deposit sample was subjected to X-Ray Diffraction (XRD) and elemental analysis. The XRD and elemental analysis results for the black debris on the reservoir filter are shown in Figure 16 and Figure 17 respectively and Table 4.

Based on the XRD results, the deposit was identified as silane based compounds. Therefore, we can eliminate brake fluid polymerization as a possible cause since no siloxane based polymers were observed. However, the debris appeared to also contain a liquid that had a very low vapor pressure and did not evaporate in a vacuum. Therefore, it was not certain if the XRD analysis detected the residual silicone brake fluid or the deposit itself. This is also indicated by a strong Si peak in the elemental analysis result. Since there appeared to be no elastomeric compounds evident from the XRD analysis, we can simply state that the material could be either silicone grease and/or residual silicone brake fluid contained in the black residue.

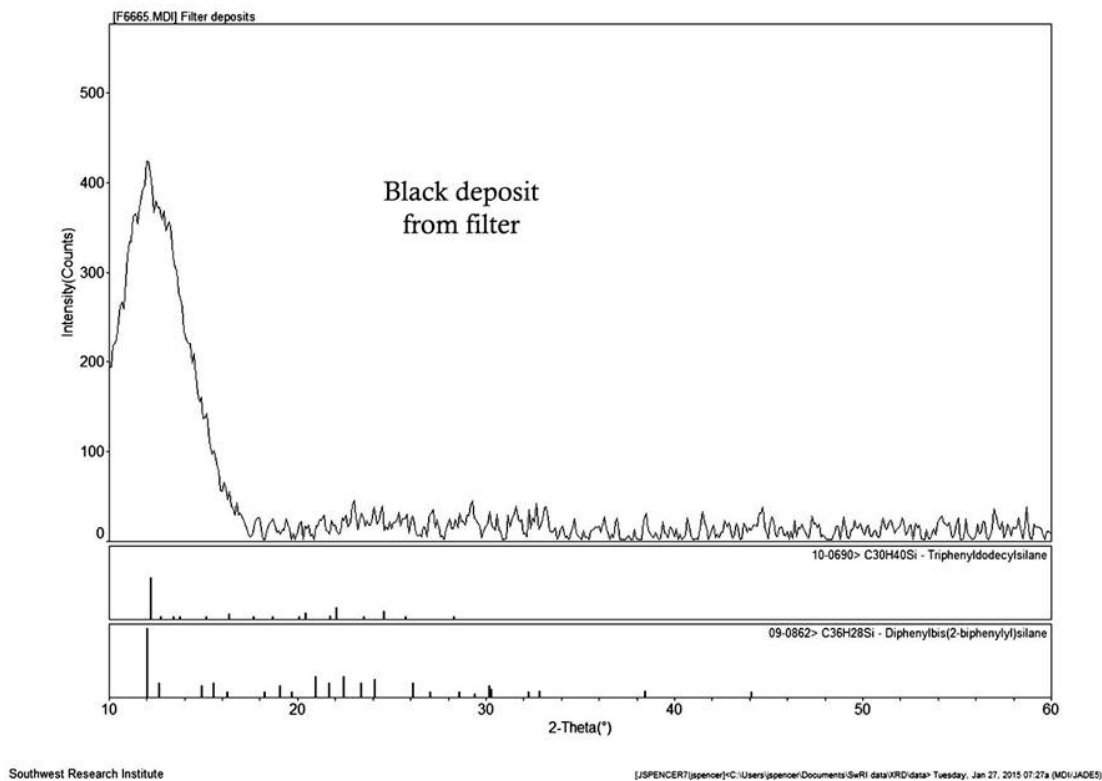


Figure 16. MIL-PRF-46176 Brake Fluid Filter Deposit

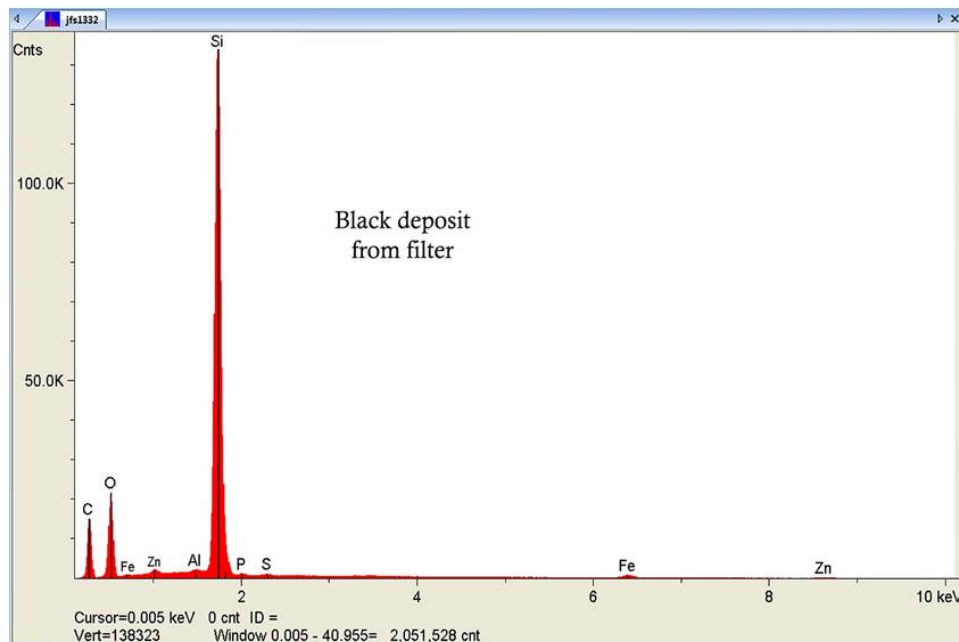


Figure 17. Filter Debris Elemental Analysis

Table 4. Elemental Analysis of Deposit

Elt.	Line	Intensity (c/s)	Atomic %	Conc.	Units
Al	Ka	43.07	0.99	0.94	wt.%
Si	Ka	3,947.01	95.79	93.90	wt.%
P	Ka	11.37	0.81	0.88	wt.%
S	Ka	12.82	0.67	0.75	wt.%
Fe	Ka	33.56	1.27	2.48	wt.%
Zn	Ka	6.90	0.46	1.05	wt.%
			100.00	100.00	wt.%

kV 20.0
Takeoff Angle 23.0°
Elapsed Livetime 300.0

In addition to the above investigation, FTIR spectra was obtained on the HPB servo valves numbered 4, 5, 6, and 10, and was compared to FTIR spectra obtained for the new silicone brake fluid. An overlay of the spectra of the servo valves and the HSF fluid is shown in Figure 18. Please note the intensity is scaled such that the differences are visible. A 0 to 100 intensity scale might not show clear differences as shown in the above FTIR spectra.

It can be observed in that the spectra from the servo valves were a match for the silicone brake fluid except, for the following peaks: 3296.91 cm^{-1} indicate presence of O-H peak corresponding

to water; 1631.50 cm^{-1} indicate presence of C=C peak corresponding to alkenes; 1531.36 cm^{-1} indicate presence of C=C peak corresponding to aromatic compounds; Multiple peaks around 1463.01 cm^{-1} indicate presence of C-H peak corresponding to alkanes.

In comparing with the identity of HBP elastomers in Table 3, it should be noted that these peaks indicate the probability of SBR elastomeric residue, where in, the C=C peak corresponding to alkenes point to butadiene chain, and C=C corresponding to aromatics point to phenyl group that matches styrene-butadiene (SBR) structure. Based on the FTIR spectra from these servo valves, there is potential evidence of SBR elastomeric residue on the servo valves. In order to confirm this inference, the used brake fluid from these servo valves have to be examined for the presence of SBR elastomeric residue. The subsequent section describes the used brake fluid analysis.

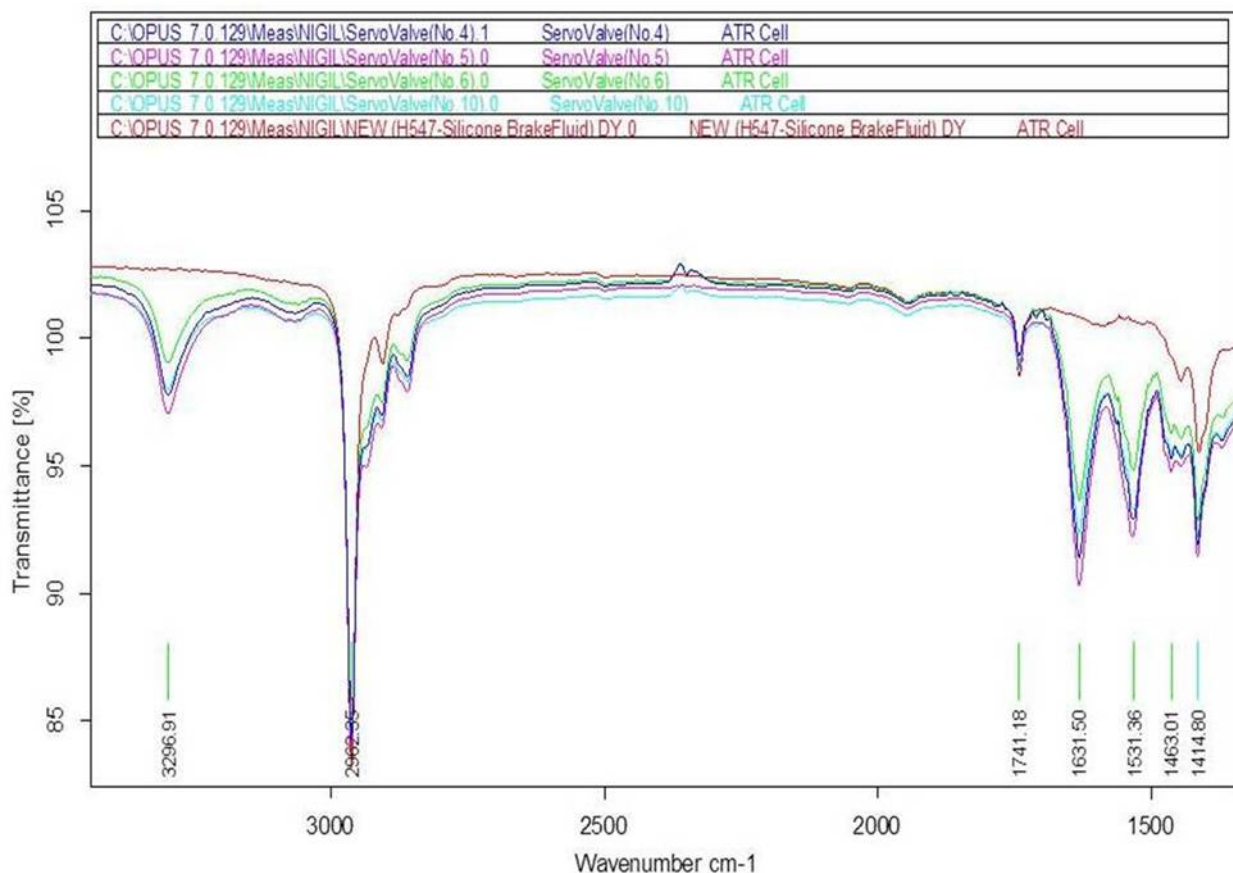


Figure 18. FTIR Spectra of Four Servo Valve Filters and Fresh Silicone Brake Fluid

3.4 USED HSF BRAKE FLUID ANALYSIS

Figure 19 shows the used HSF fluid that was filtered for analysis. Elemental analysis of scraped material from this filter paper, shown in Figure 20 and Table 5 confirms a high amount of Si that could be potentially from the brake fluid. Therefore, in order to determine the presence of elastomer in the residue, the scraped material was subjected to SEM imaging which would confirm the physical presence of elastomers, followed by subjecting the residue to XRD which would confirm the actual chemical identity if the elastomer were present.



Figure 19. Filtered Residue from Used HSF

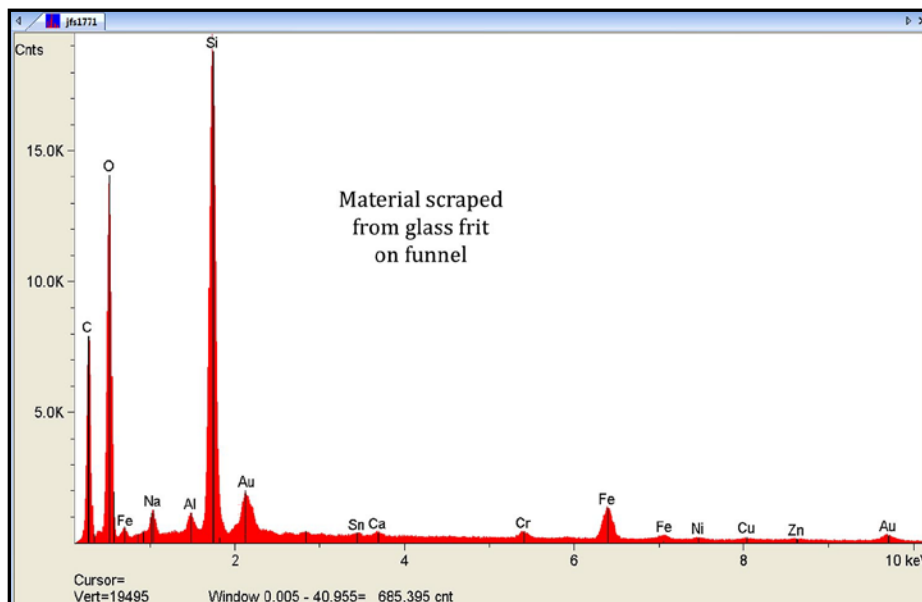


Figure 20. Elemental Analysis of Filtered Residue from used HSF

Table 5. Relative Elemental Concentration of Residue from used HSF

Elt.	Line	Intensity (c/s)	Atomic %	Conc	Units	
Na	Ka	15.81	5.59	4.02	wt.%	
Al	Ka	19.41	3.13	2.64	wt.%	
Si	Ka	543.29	77.22	67.82	wt.%	
Ca	Ka	4.17	0.49	0.61	wt.%	
Cr	Ka	10.96	1.37	2.22	wt.%	
Fe	Ka	56.34	8.63	15.08	wt.%	
Ni	Ka	4.73	0.95	1.75	wt.%	
Cu	Ka	4.65	1.09	2.16	wt.%	
Zn	Ka	4.23	1.18	2.40	wt.%	
Sn	La	3.91	0.35	1.30	wt.%	
			100.00	100.00	wt.%	Total

kV 20.0

Takeoff Angle 23.0°

Elapsed Livetime 300.0

Note: Results do not include elements with Z<11 (Na).

SEM images shown in Figure 21 indicate the presence of threaded structures in addition to solid agglomerate residue indicating the physical presence of elastomer/polymer threads. XRD results in Figure 22 indicate the presence of two chemical structures, namely, 1,4-diphenyl-1,3-butadiene which indicate the presence of Styrene-Butadiene Rubber (SBR), and N-phenylmaleimide which this compound was used for grafting polymers at low concentrations and was used in a 'diene' which point out to EPDM or SBR. Thus, XRD results confirm the

presence of SBR in the residue obtained by filtering the used brake fluid. N-phenylmaleimide also confirms that the oxygen peak in elemental analysis comes from this compound.

Based on the collective physical and chemical characterization, it can be inferred that there was SBR elastomer presence in the used silicone brake fluid residue and that there was a fine SBR elastomer layer coated on the surface of the servo valves. Based on FTIR characterization of elastomers and the above results, it can be concluded that the elastomers could have come from any of the following components: Parking Brake Supply (valve body seal), Relay Valve Seal, Pump Plunger Dynamic Seal or Reservoir Seal, with the pump plunger dynamic seal being the highly likely location from which SBR elastomer could have been leached into the brake fluid due to dynamic motion. For future work, it is recommended that Raman measurements be conducted on these elastomers and on residues, if feasible.

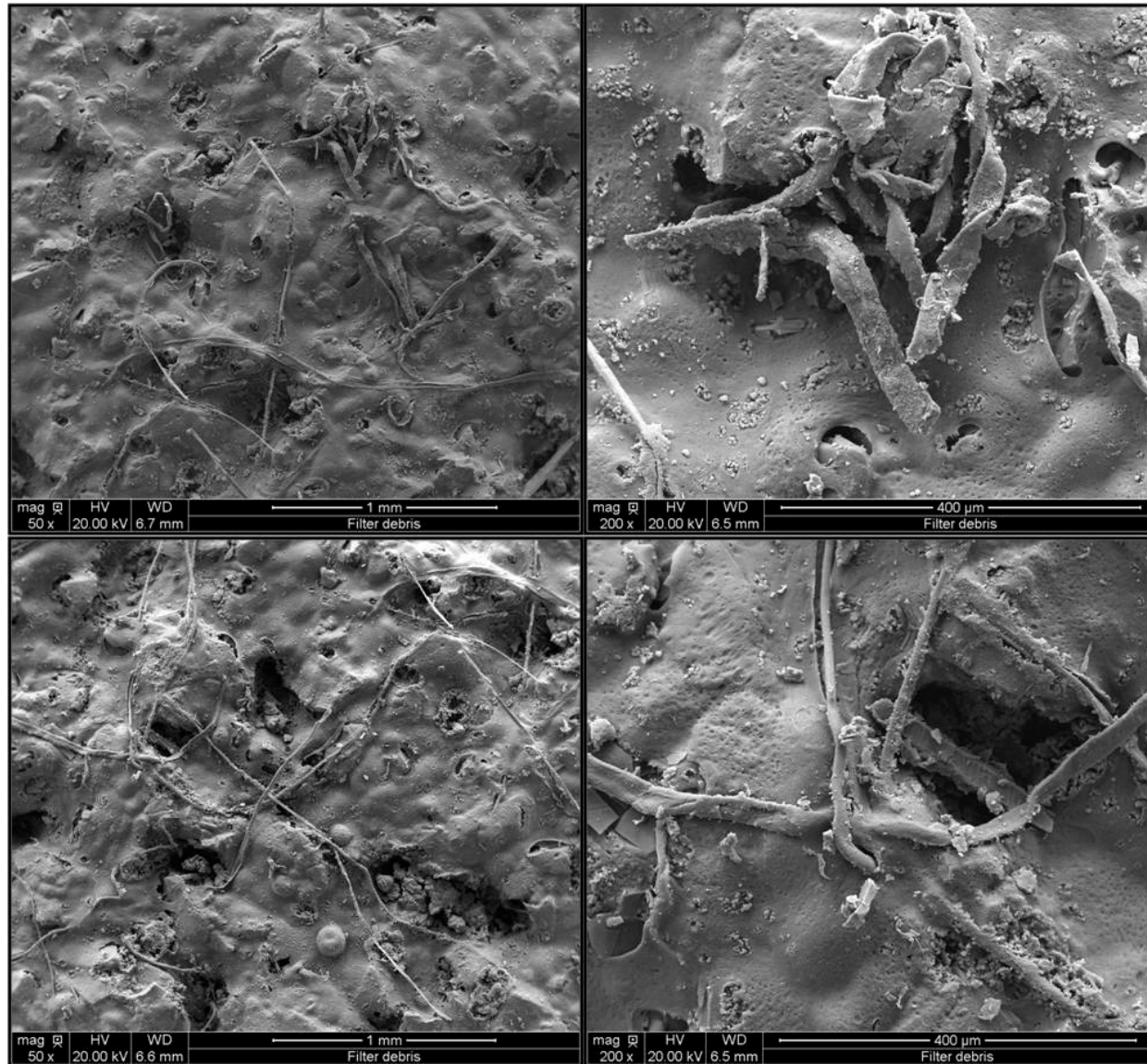


Figure 21. SEM Images of the Filtered Residue

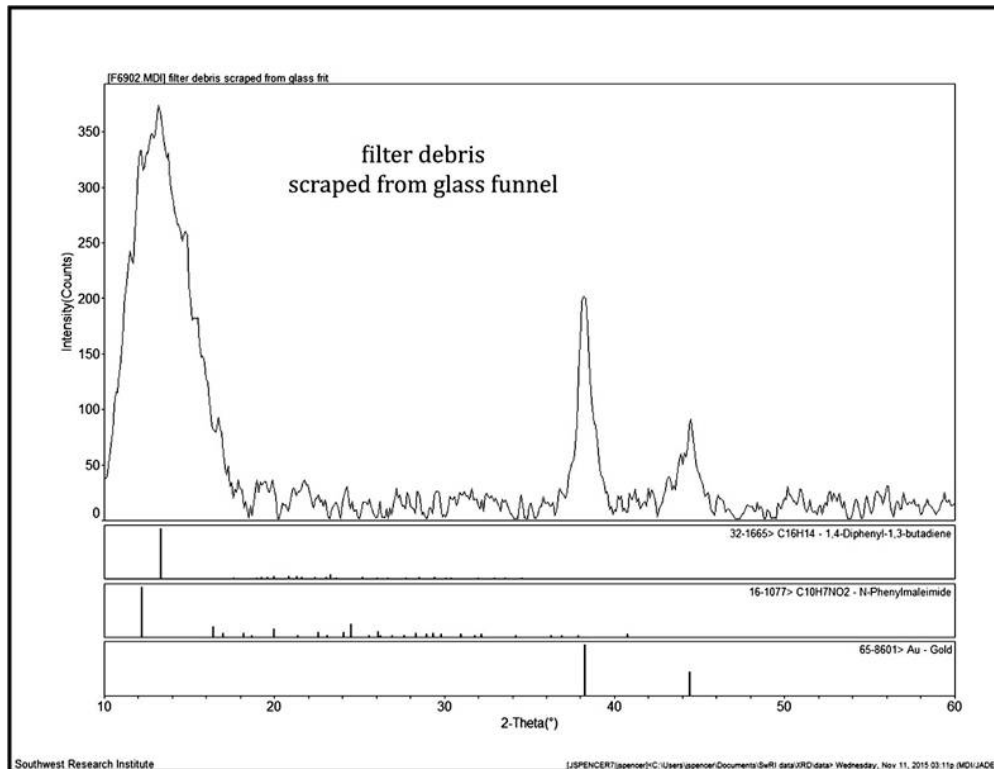


Figure 22. XRD Results of the Filtered Residue

4.0 Hydraulic Power Brake Unit Hardware Analysis

4.1 HYDRAULIC POWER BRAKE PUMPING ELEMENT ANALYSIS

The Hydraulic Power Brake (HPB) units that had undergone 20,000-cycles of testing with the HSF (MIL-PRF-46176) and the baseline (SAE J1703 DOT 3) brake fluids were disassembled for inspection of the internal component conditions. Each HPB unit had two pumping elements, noted as LR and LF, that were serviceable items and easily removed. In addition each HPB unit had ten servo valves that were swaged in place and required destructive efforts to remove.

The two pumping elements from the HSF test article were disassembled and inspected for wear patterns. The disassembled components of a pumping element are shown in Figure 23. A close up image of the pumping element plunger is displayed in Figure 24. There appeared to be some polishing wear on the large diameter sections, some of which can be seen on the left side of the plunger. The wear on the right side of the plunger was diametrically opposite, to the right of the black seal.



Figure 23. Disassembled Hydraulic Power Brake Pumping Element



Figure 24. Hydraulic Power Brake Pumping Plunger Detail

The barrels and plungers from the HSF test were sent for high resolution imaging, with the barrels cut in half using WEDM for surface analysis. The HPB unit that was used for the baseline fluid testing was also disassembled for comparison of the pumping plungers.

The barrels and plungers from both the HSF and baseline tests were photographed under higher magnification and are shown below for comparison. Figure 25 shows the overall condition of the

HSF LF plunger with wear seen on both the pumping (left) end and the follower (right) end. The baseline plunger condition is shown in Figure 26, each operated for 20,000 cycles. A closer image of the HSF plunger pumping section wear is shown as Figure 27 and the baseline plunger in Figure 28. There appeared to be less polish on the baseline LF plunger. Magnification of the HSF LF plunger follower wear is shown in Figure 29, where towards the left edge of the image, distress to the elastomeric seal was observed. The baseline LF plunger follower wear is shown in Figure 30, where towards the left edge of the image, very little distress to the elastomeric seal were observed. The area around the follower end is only lubricated by fluid that is wiped onto the barrel bore by the seal, as these sections were dry when disassembled.

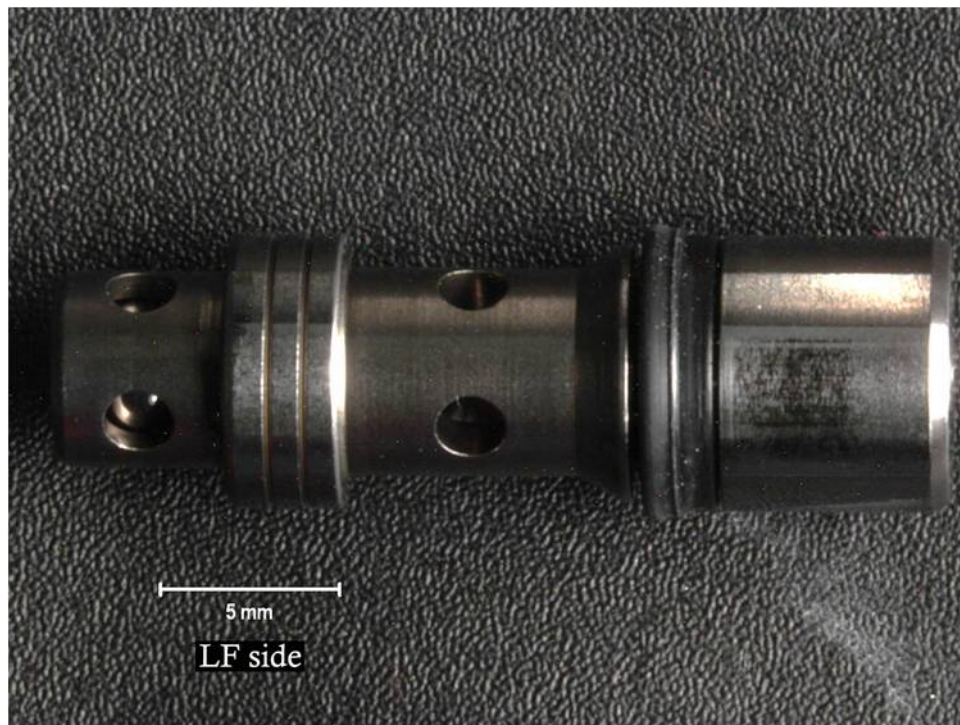


Figure 25. LF Plunger Overview from HSF Testing

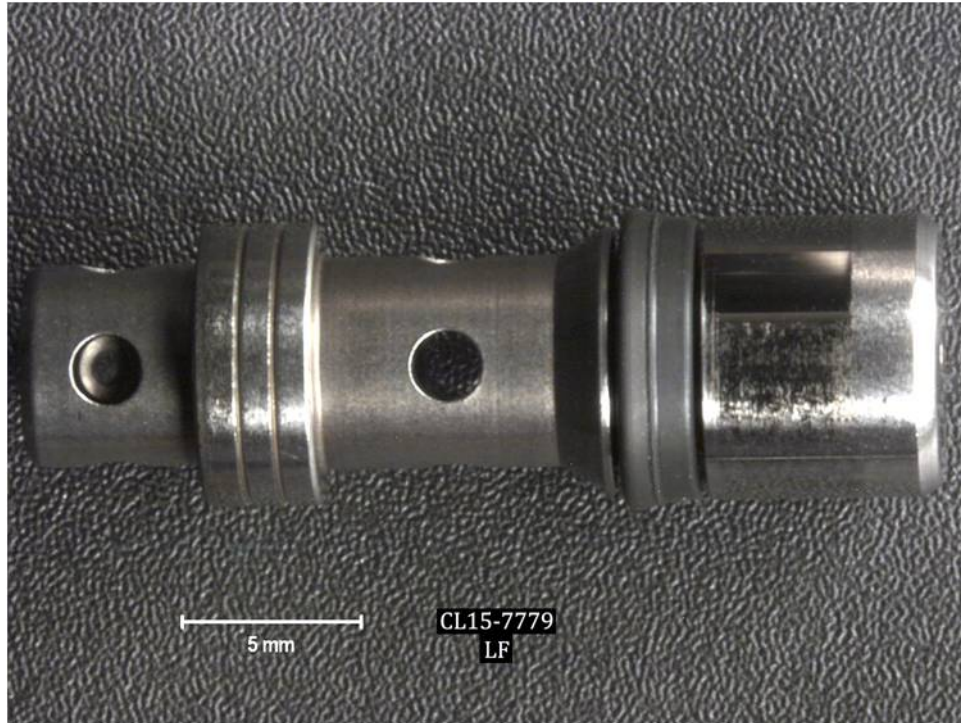


Figure 26. LF Plunger Overview from Baseline Testing

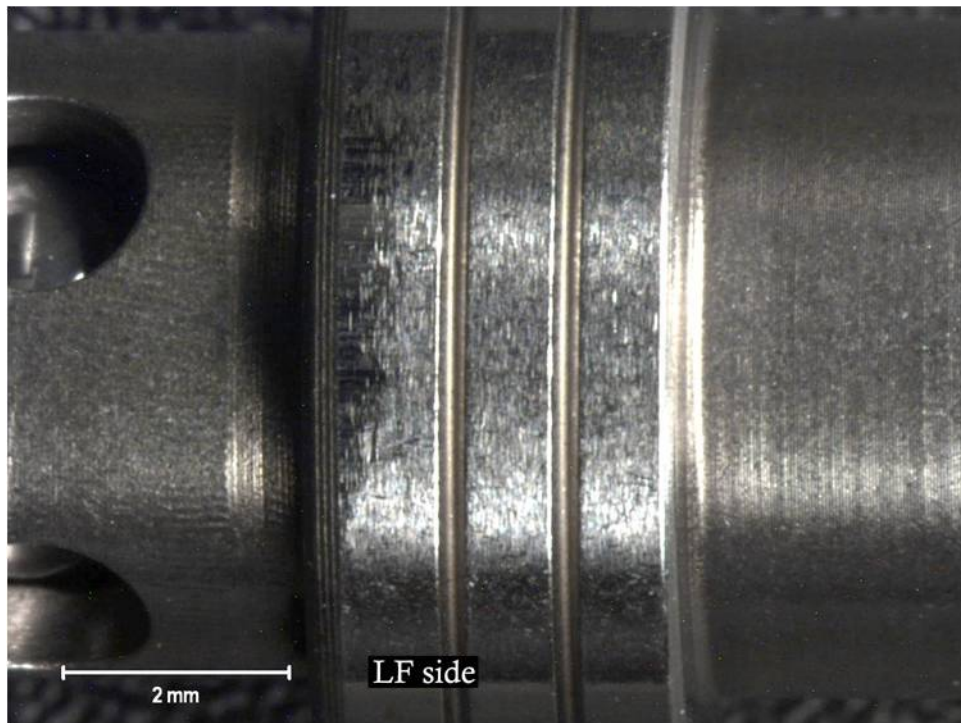


Figure 27. Detail of the HSF LF Plunger Pumping Section Polishing and Wear



Figure 28. Detail of the Baseline LF Plunger Pumping Section Polishing and Wear

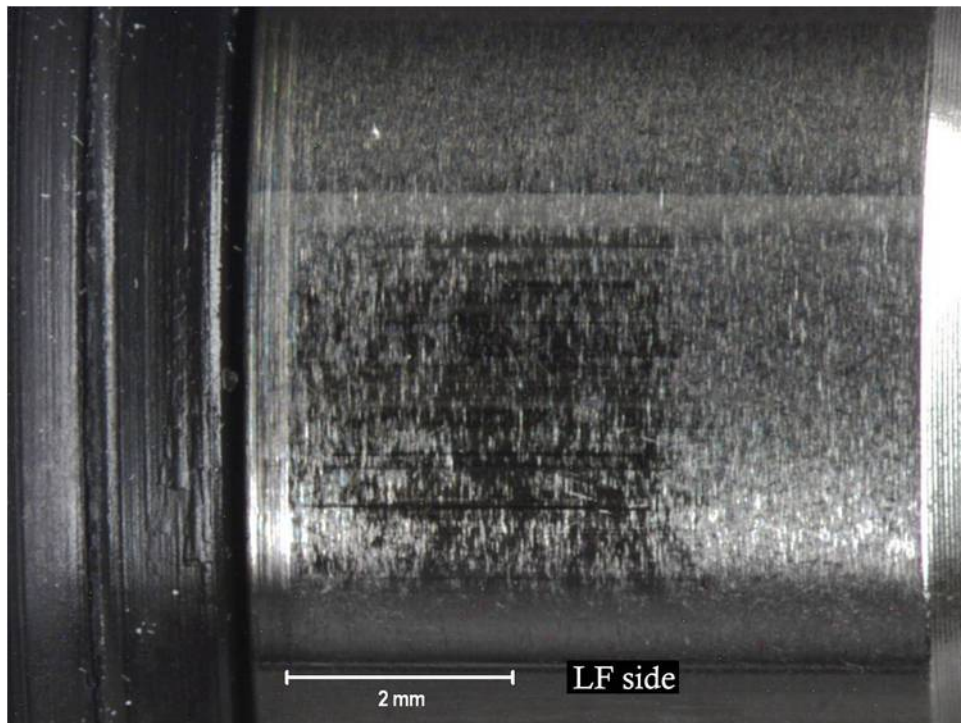


Figure 29. Close up of the HSF LF Plunger Follower Section Polishing and Wear

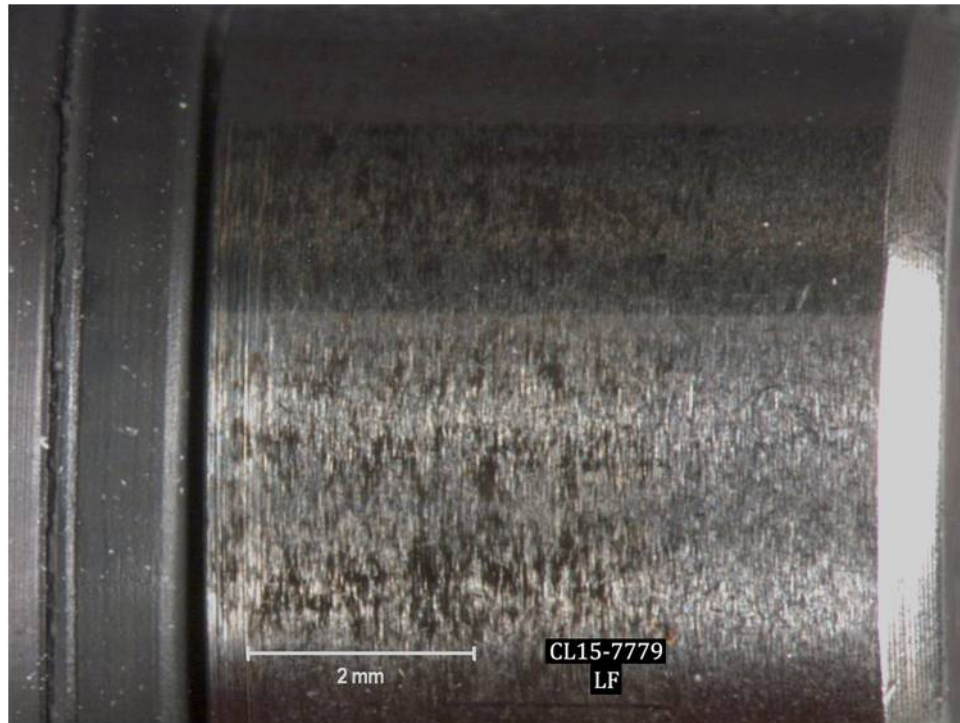


Figure 30. Close up of the Baseline LF Plunger Follower Section Polishing and Wear

The LF pumping element barrel was cross-sectioned using Wire Electrostatic Discharge Machining (WEDM). The wear between the piston follower section and the barrel are shown in Figure 31 towards the left edge of the image for the HSF LF pumping element barrel. The corresponding baseline LF barrel shows very little wear as seen in Figure 32. A closer view of the elastomer distress for the HSF fluid is shown in Figure 33. It is postulated that debris from the barrel/plunger wear at the follower end was what caused the elastomer distress. A closer view of the elastomer distress for the baseline fluid is shown in Figure 34.

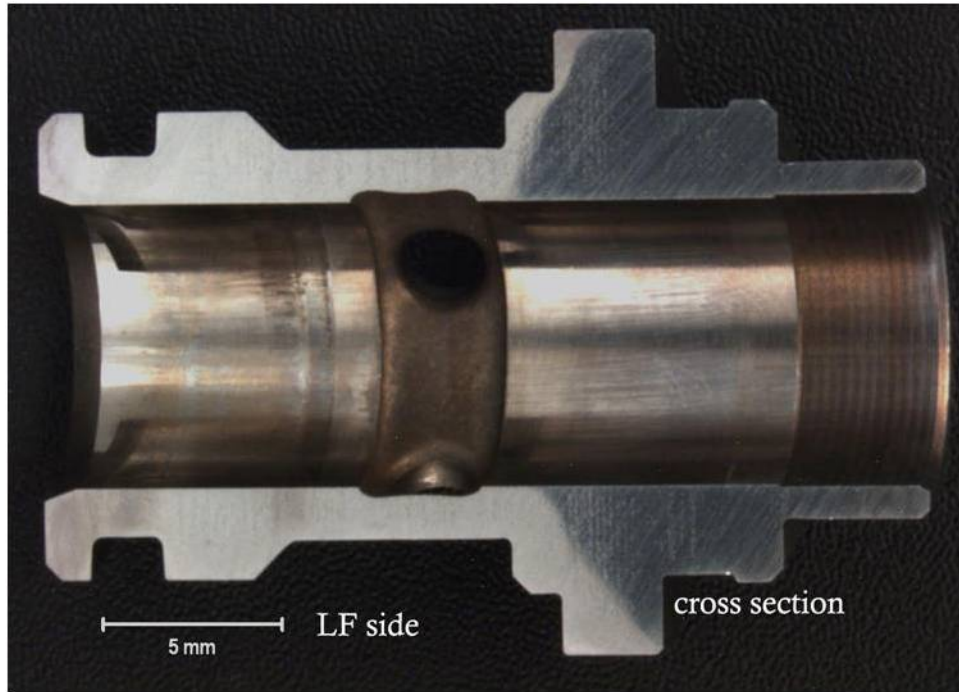


Figure 31. Sectioned HSF LF Barrel with Bore Wear from Follower

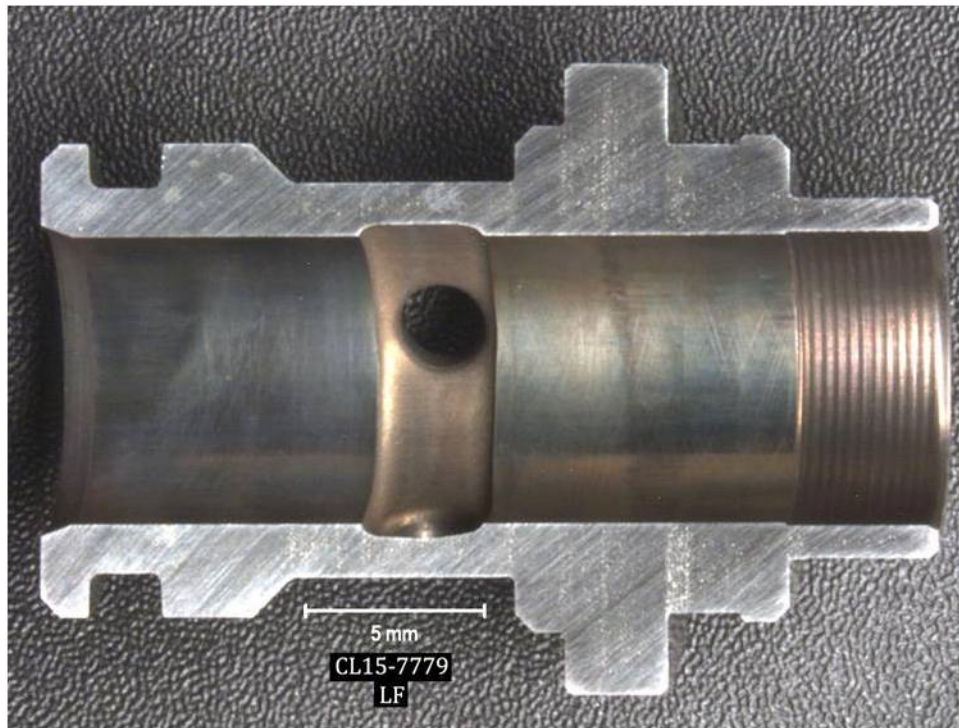


Figure 32. Sectioned Baseline LF Barrel with Bore Wear from Follower

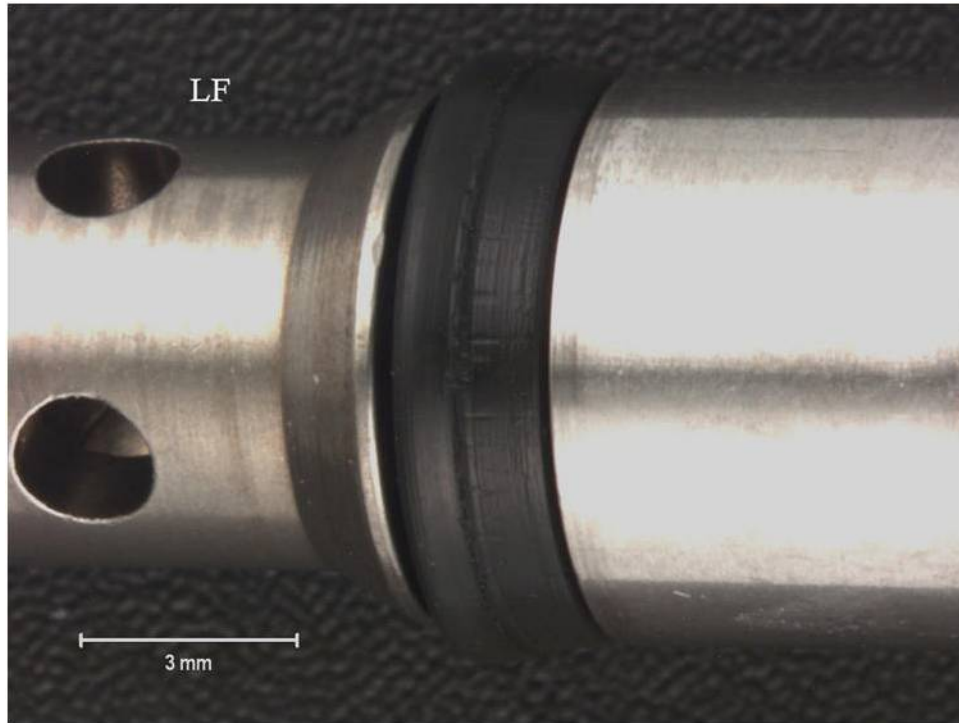


Figure 33. Elastomer on LF Plunger from HSF Testing

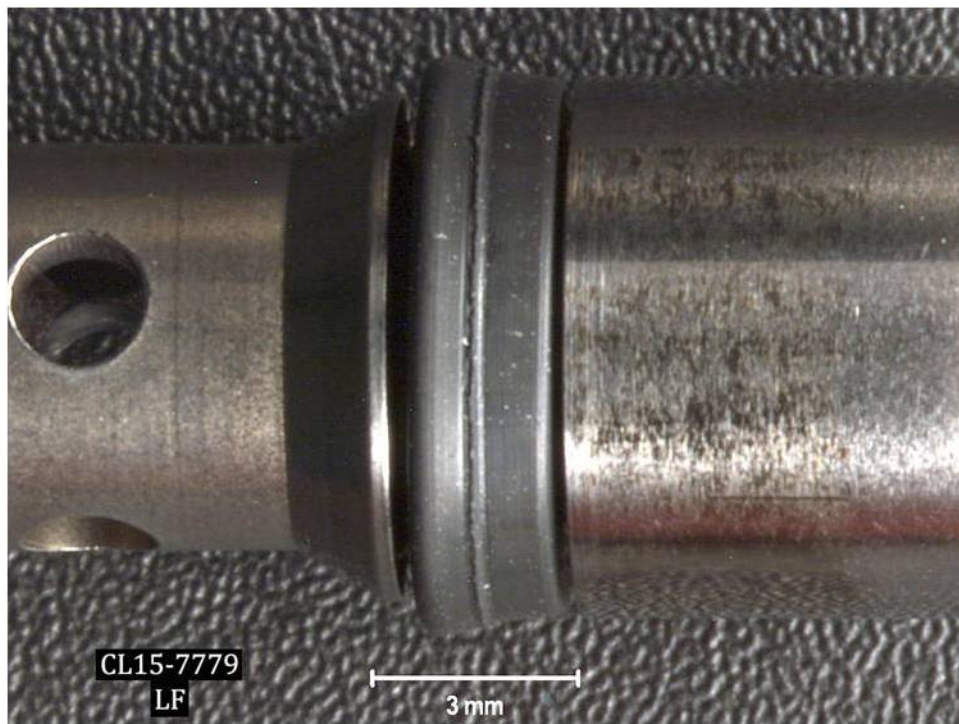


Figure 34. Elastomer on LF Plunger from Baseline Testing

The overall condition of the HSF LR plunger is seen in Figure 35, with wear seen on both the pumping (left) end and the follower (right) end. More wear was evident on the LR plunger after HSF testing. The baseline LR plunger is shown in Figure 36 with very little polishing evident. A closer image of the HSF LR plunger pumping section wear is seen in Figure 37, and the similar baseline LR plunger section in Figure 38. Magnification of the HSF LR plunger follower wear is shown in Figure 39, where towards the left edge of the image distress to the elastomeric seal was also observed as before. The wear on the baseline LR plunger was minimal and the elastomer distress was also minimal as seen in Figure 40. More wear was evident on the LR plunger than the LF plunger, especially on the follower section, with the HSF brake fluid. Again it appeared the area around the follower end was only lubricated by fluid that was wiped onto the barrel bore surface by the seal. For the baseline fluid, the LR and LF plunger wear was similar. There was more overall plunger wear with the HSF fluid than the baseline fluid.

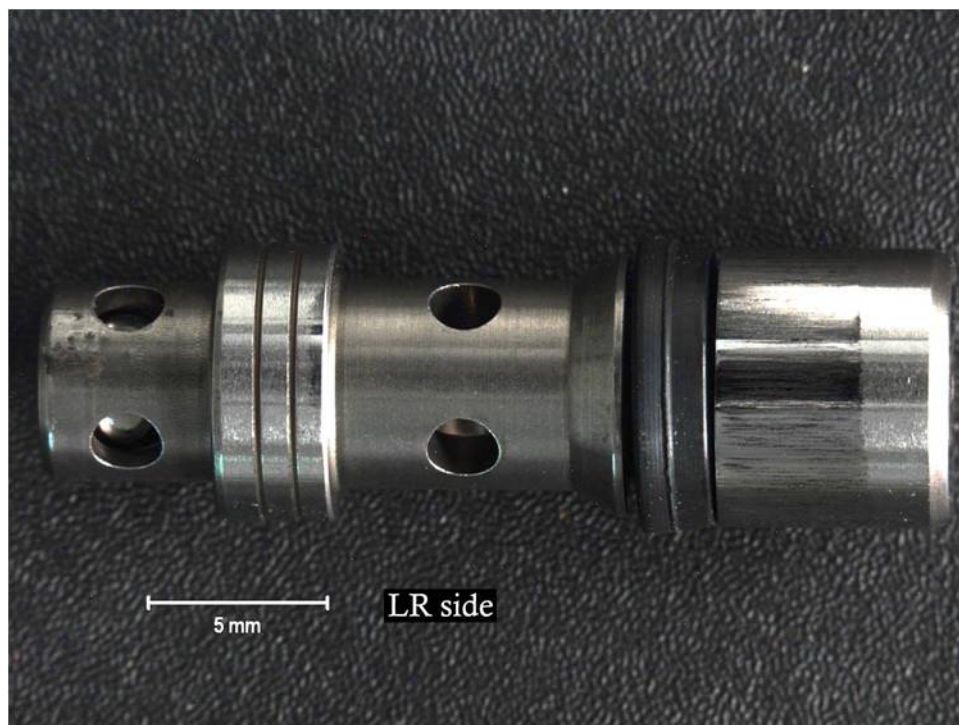


Figure 35. LR Plunger Overview from HSF Testing

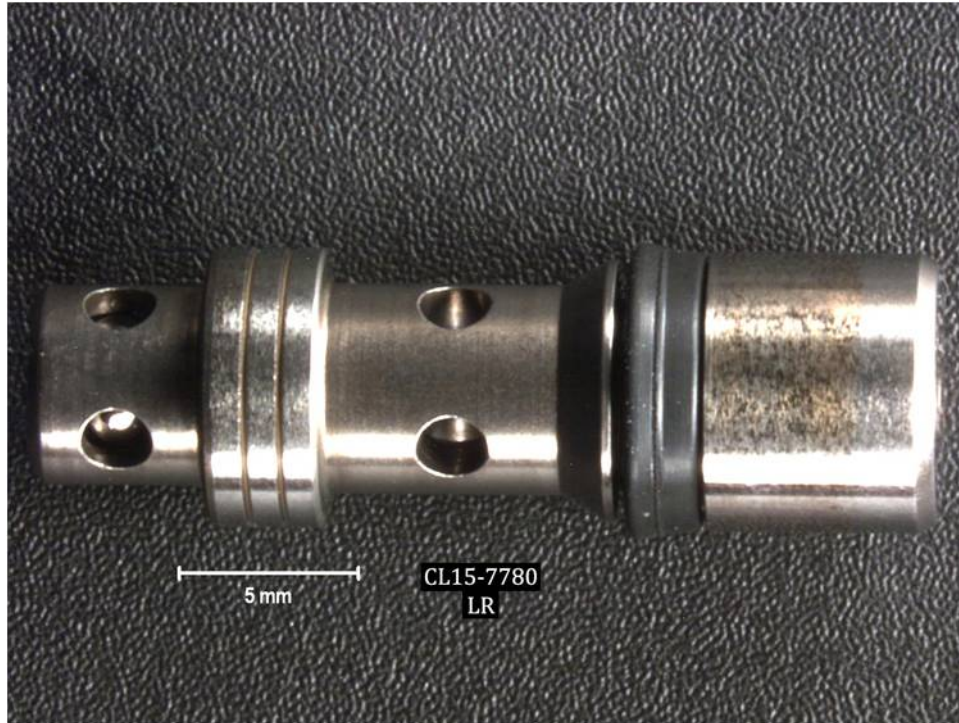


Figure 36. LR Plunger Overview from Baseline Testing

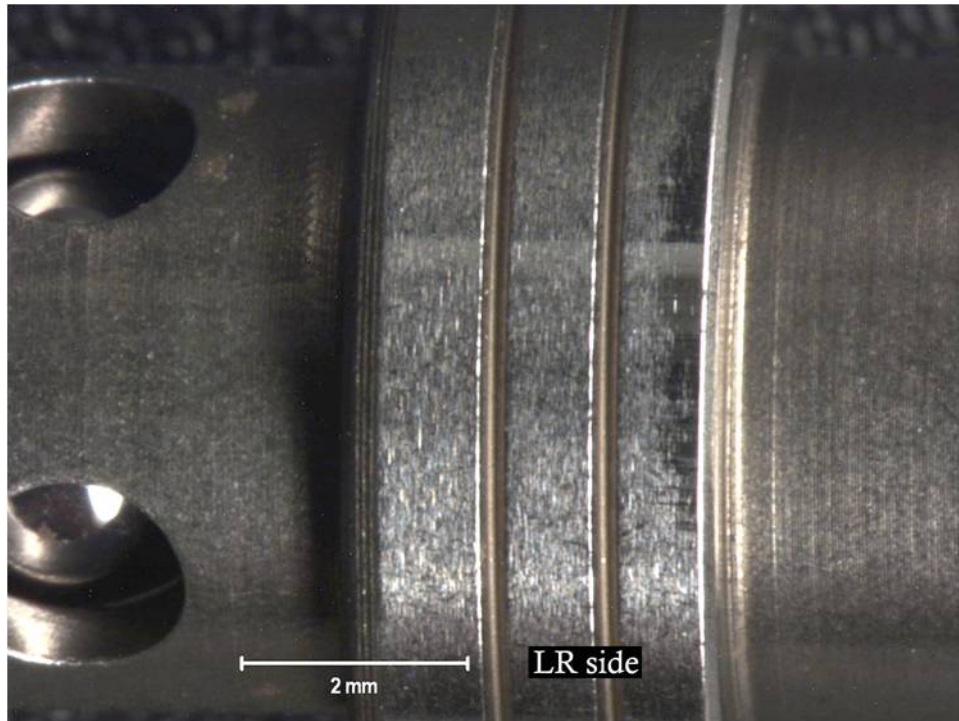


Figure 37. Detail of the HSF LR Plunger Pumping Section Polishing and Wear

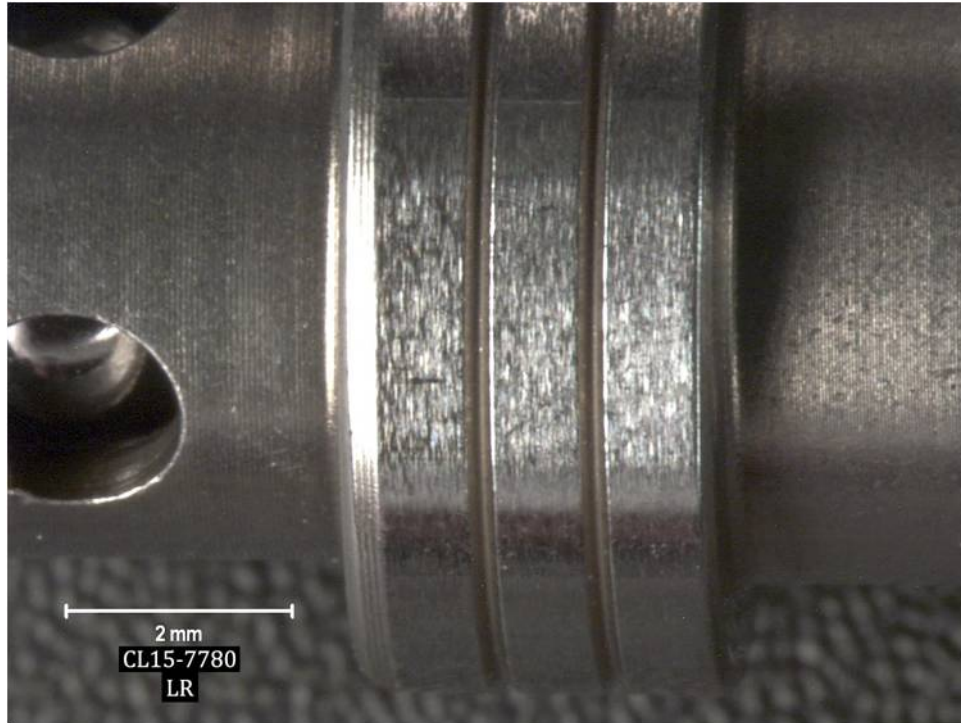


Figure 38. Detail of the Baseline LR Plunger Pumping Section Polishing and Wear

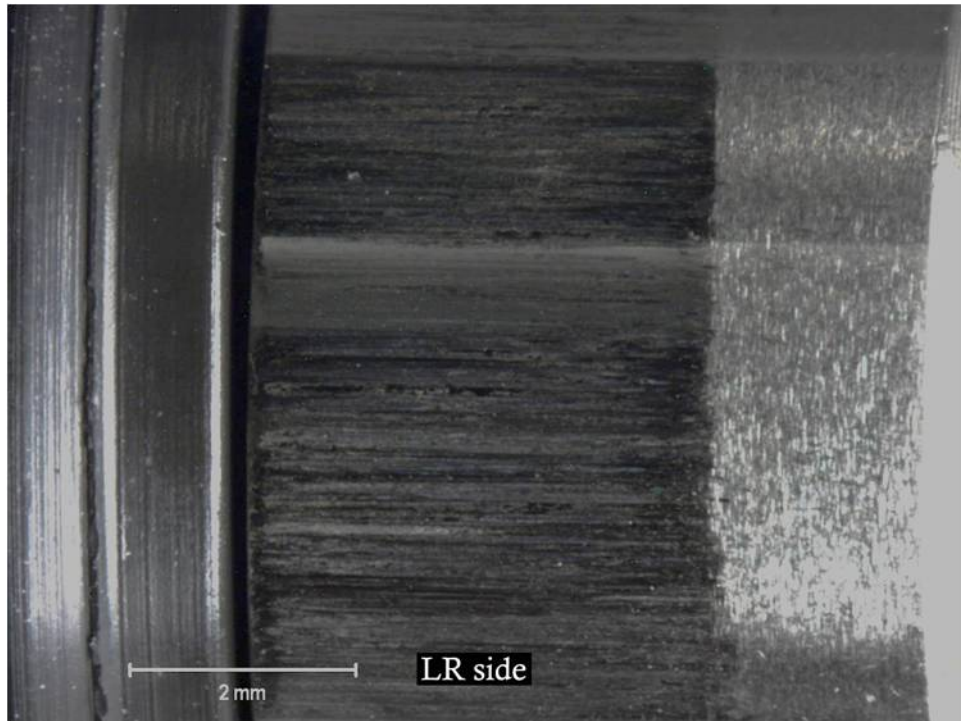


Figure 39. Close up of the HSF LR Plunger Follower Section Polishing and Wear

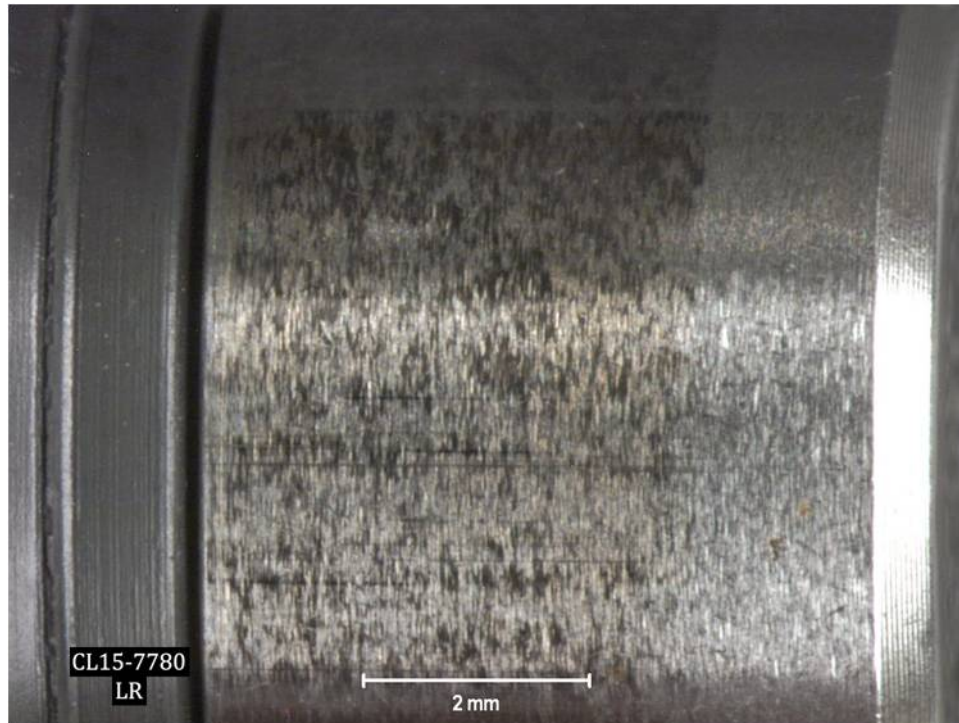


Figure 40. Close up of the Baseline LR Plunger Follower Section Polishing and Wear

The LR pumping element barrel was also cross-sectioned using WEDM. The wear between the piston follower section and the barrel are shown in Figure 41 for the HSF fluid. Towards the left edge of the image for the LR pumping element barrel scuffing and material transfer was evident. The corresponding baseline LR barrel shows very little wear as seen in Figure 42. A closer view of the elastomer distress is shown in Figure 43. It appears evident debris from the barrel/plunger wear at the plunger follower section caused the elastomer distress. A closer view of the minimal LR plunger elastomer distress for the baseline fluid is shown in Figure 44.

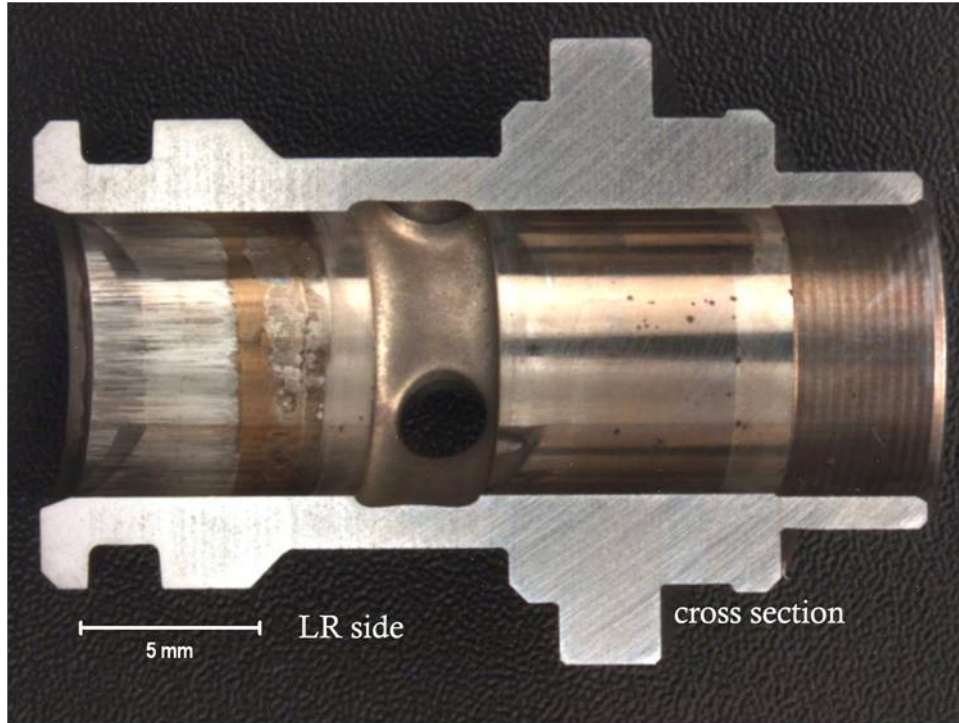


Figure 41. Sectioned HSF LR Barrel with Bore Wear from Follower

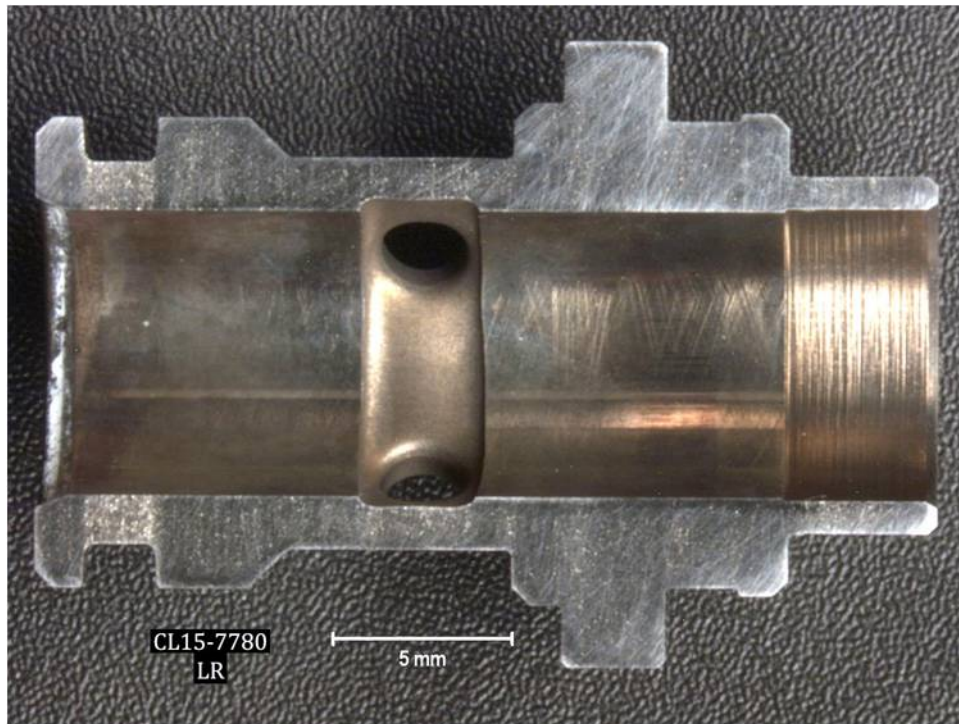


Figure 42. Sectioned Baseline LR Barrel with Bore Wear from Follower

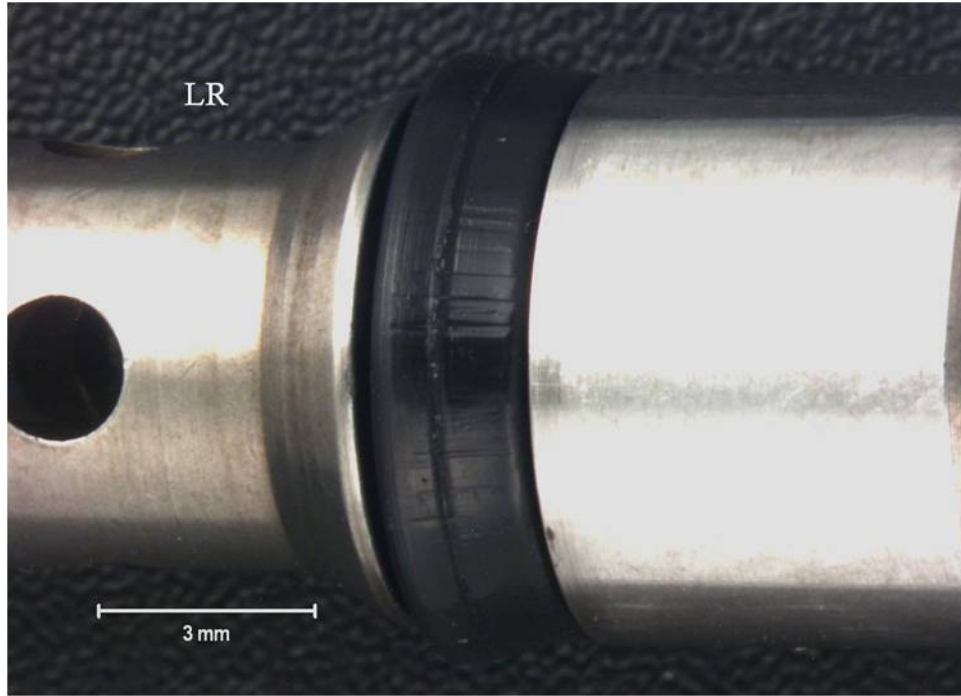


Figure 43. Elastomer on LR Plunger from HSF Testing

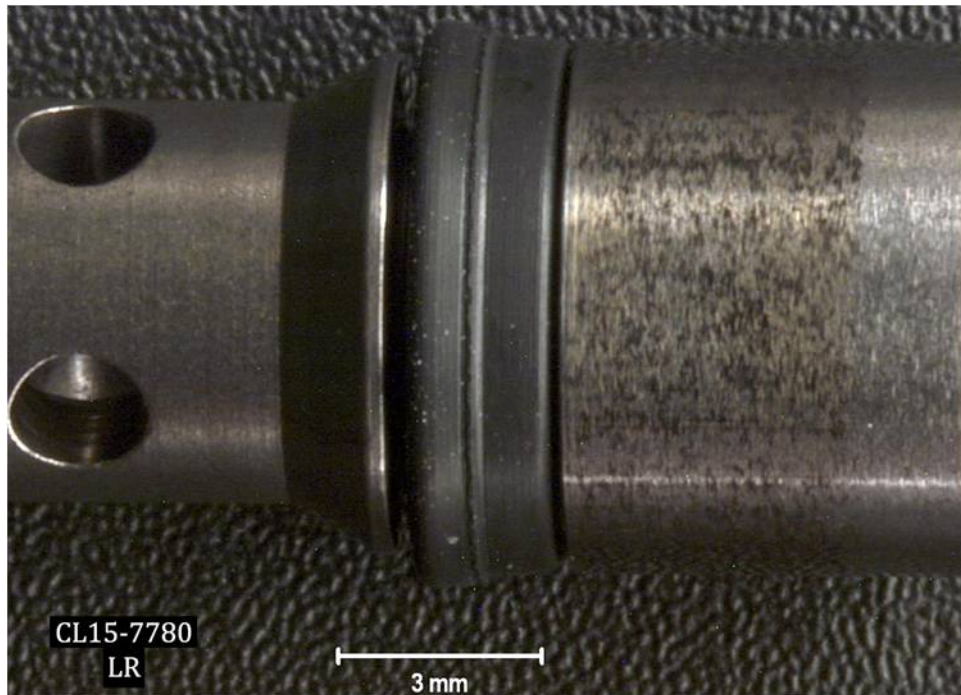


Figure 44. Elastomer on LR Plunger from Baseline Testing

Overall it was observed that the HPB unit utilized for HSF brake fluid testing had more elastomer distress and more wear than the unit used for the baseline brake fluid testing.

4.2 HYDRAULIC POWER BRAKE SERVO VALVE REMOVAL

Efforts were made to remove the servo valves from the HPB block used for HSF testing using heat and dry ice. It was determined by cutting up a spare HPB, that the valves had been swaged into the machined port during assembly making it impossible to remove them by pushing, pulling, or heating. The parts needed to be cut out of their enclosures.

The following figures document how the servo valves and filters were removed from the HPB block. Figure 45 shows how the valve section was sliced off the HPB block with a band saw. The slice with the band saw was below the depth of the servo valve machining. The valves were numbered individually as shown in Figure 46, then parallel cuts were made between valve rows. Each valve was then isolated by making cuts perpendicular to the row cuts as shown in Figure 47.



Figure 45. Valves sliced from the main block using a band saw



Figure 46. Parallel cuts were made along each row, with valves numbered as indicated



Figure 47. Cuts were then made perpendicular to the row cuts to isolate each valve and filter unit

After each valve was isolated, three notches were made around each individual valve body, Figure 48, to assist with valve removal. A hammer and chisel was then used to separate the aluminum body from the valve as shown in Figure 49. The filters from servo valve bodies 4,5,6, and 10 bodies were analyzed using FTIR as discussed previously.



Figure 48. Small cuts were made on 3 sides as indicated



Figure 49. A hammer and chisel was then used to crack open the case and the valve and filter were then removed

5.0 Brake Fluid Properties and Lubricity

Brake fluid samples were analyzed for density at 15 °C, and for kinematic viscosity at three temperatures. The samples analyzed included untested samples of both baseline (SAE J1703) and HSF (MIL PRF-46176) fluids, both fluids after being cycled through a Hydraulic Power Brake system, and a newly obtained fresh sample of HSF. The stock of HSF fluid had changed to a yellowish color, from the originally dyed purple color. It was felt this may be due to oxidation, as this color change had been previously noted when small samples of fluid were left exposed to the atmosphere. A fresh HSF sample from an Army Reserve Unit stationed at Fort Sam Houston in San Antonio, TX was obtained to determine if fluid property results changed between fresh and aged HSF fluids.

The density and kinematic viscosity results are shown in Table 6 for the fluids analyzed. Both types of fluids had similar densities, with the baseline fluid being the densest. The baseline brake fluid viscosity revealed a large variation of viscosity with temperature, whilst all the HSF samples revealed substantially smaller effects of temperature on viscosity. The lower temperature sensitivity of the HSF fluids suggests brake system performance with the HSF fluid should be more consistent across a broad temperature range.

Table 6. Brake Fluid Property Analysis

Brake Fluid	Sample ID	Density, ASTM D4052 @15°C, kg/m ³	Kinematic Viscosity, ASTM D445		
			-55°C, mm ² /s	-40°C, mm ² /s	100°C, mm ² /s
Baseline	CL15-8253	1036.6	11779.4	1188.4	1.99
Cycled Baseline	CL15-8810	1002.0	11519.8	1167.8	2.00
HSF	CL15-8255	970.5	642.0	295.6	13.32
Cycled HSF	CL15-8254	966.2	589.3	276.3	13.20
Fresh HSF	CL15-8728	970.7	637.7	294.1	13.06

Samples of the fresh baseline brake fluid, the cycled baseline fluid, the HSF fluid, the cycled HSF fluid, and an additional fresh HSF fluid were submitted for bench wear tests. The tests performed were the ASTM D5001 BOCLE test and the ASTM D6078 HFRR test at 60 °C. Bearing in mind these bench tests were developed for lubricity characterization of aviation fuels and diesel fuels respectively, the results from the brake fluids tests were not that indifferent from good fuels. The

results are shown in Table 7. The higher viscosity of the brake fluids than fuels were anticipated to have a greater effect on the results, in the form of much smaller wear scars than fuels. The BOCLE tests suggest the HSF fluids are slightly more severe than the baseline fluid. The fresh sample of HSF from Fort Sam Houston revealed the largest BOCLE wear scar. Of interest with the HFRR results is how severe the cycled HSF fluid appeared compared to the fresh HSF and baseline fluids. The increased wear seen on the system pumping plungers, and corresponding barrels, with the HSF in the HPB testing appear to correspond to the HFRR wear result.

Table 7. Bench Wear Test Results for Brake Fluids

Brake Fluid	Sample ID	ASTM D5001 BOCLE, mm	ASTM D6078 HFRR, mm
Baseline	CL15-8253	.511	.338
Cycled Baseline	CL15-8810	.483	.302
HSF	CL15-8255	.535	.281
Cycled HSF	CL15-8254	.521	.430
Fresh HSF	CL15-8728	.665	.361

6.0 CONCLUSIONS

The overall conclusion is that the root cause of deposit buildup in the system reservoir, that caused testing with silicone brake fluid to halt in FY13, is due to formation of a thin Styrene-Butadiene (SBR) elastomer residue on the servo valves. This conclusion has been substantiated through a number of conclusions from static soak and dynamic seal tests, hydraulic power brake system teardown, followed by a series of conclusions from physical and chemical characterization tests.

The two HPB systems that had undergone cyclic testing with HSF and the baseline brake fluids were dismantled to ascertain component conditions. The pumping elements from each HPB were removed and cross-sectioned to document wear. The pumping elements exposed to HSF had more severe wear on the pump pistons, piston dynamic seals, and pump barrels. Bench top lubricity tests, usually utilized for fuel lubricity measurements, confirmed that HSF had lower lubricity than the baseline brake fluid. In particular the HSF that had been cycled in the HPB revealed the lowest lubricity. The lower lubricity of HSF combined with HSF effect on seal components lead to increased pump wear, corresponding increased elastomer wear, and the subsequent brake system debris.

Analysis of used HSF fluid from static soak test results using GC-MS indicated the absence of any elastomer residue. The conclusion from static soak tests was that SBR did not leach into the silicone brake fluid at static conditions. Hence, the chemical constituents in the silicone brake fluid was not a primary factor for SBR dissolution into the brake fluid. However, property analysis of SBR elastomer from static soak test at 40 °C indicated that the silicone brake fluid lowered the tensile strength of the SBR elastomer by 16.67%. The conclusions from dynamic seal tests indicated that dynamic motion of SBR elastomer in HSF fluid cause increase in thickness by approximately 6%, made the elastomer softer by approximately 10% by absorbing silicone brake fluid, increasing weight by about 8% and volume swell by about 13%. Such increase in all physical properties indicate that SBR material could be subject to potential wear when there is dynamic motion.

FTIR tests of all the HBP elastomers lead to the conclusion that SBR dissolution into the silicone brake fluid could have come from the Pump Plunger Dynamic Lip Seal. Analysis of solid residue in the reservoir by FTIR and elemental analysis concluded that the presence of silicone grease and the silicone brake fluid in the deposit rather than SBR elastomer. The analysis of servo valves using FTIR led to the conclusion that the spectral bands pointed to bonds corresponding to butadiene and phenyl groups corresponding to SBR. Analysis of used brake fluid using SEM imaging indicated the presence of physical threaded structures in addition to agglomerates indicating presence of polymer structures. This was confirmed from the XRD and elemental analysis conclusions that the chemical structure was in fact 1,4-Diphenyl-1,3-butadiene, which is the repeating monomer unit in the SBR polymer/elastomer. Future research should focus on minimizing dissolution of SBR elastomer from the HBP dynamic seal, either through engineered elastomers that are wear resistant or by modifying the lubricity of the silicone brake fluid.

TFLRF investigated technical literature for corrosion studies for brake fluids in anticipation to future fluid requirements for ARMY anti-lock brake systems that will require SAE J1703 fluids. A corrosion enhanced DOT 5.1 fluid is a possible future brake fluid for advanced ARMY braking systems in lieu of MIL-PRF-46176 fluids.

7.0 REFERENCES

1. Yost, D. M., Frame, E. A., “Brake Fluid Compatibility With Hardware,” Interim Report TFLRF No. 445, prepared for U.S Army TARDEC, Force Projection Technologies, Warren, MI, 2013.
2. Johnson, J E., Frame, E., and Moses, C., “Design and Operation of a Device for Evaluating Shaft Seals in Dynamic Applications,” Interim Report TFLRF No. 371, prepared for U.S Army TARDEC, Force Projection Technologies, Warren, MI, 2003.

APPENDIX A.
ELASTOMER PROPERTY MEASUREMENTS

Thickness of the o-ring is measured using a CDI micrometer instrument (model LG2110), as shown in Figure A-1. The micrometer can measure o-rings that are up to one inch thick. The pressure foot is lifted using a lever mechanism and is positioned on the center of the o-ring. The pressure foot is lowered gradually until it comes into contact with the o-ring, and the digital reading is recorded as the thickness of the o-ring. Measurements are repeated in triplicates, and the average thickness measurement is recorded.



Figure A-1. CDI Micrometer to Measure O-ring Thickness

The hardness of the elastomer material is rated using Shore M hardness on a scale from 0 to 100. The hardness scale is indicative of the elastic modulus (Young's Modulus) of the o-ring and is a measure of the stiffness of the material. Hardness measurements are recorded using Shore M Durometer (model 714). The Shore M durometer (as shown in Figure A-2) is used to collect accurate, repeatable hardness readings on soft elastomers that are too thin or too irregular in shape for measurement with a standard durometer, such as small o-rings. It is used for cross-sections 1.25 mm – 7 mm.



Figure A-2. Shore M Durometer to Measure O-ring Hardness

The Shore test uses a hardened indenter, an accurately calibrated spring, a depth indicator, and a flat presser foot. The indenter protrudes from the middle of the presser foot and extends 2.5 mm from the surface of the foot. In the fully extended position, the indicator displays zero. When the indenter is depressed flat and is even with the presser foot's surface, the indicator displays 100. Therefore, every Shore point is equal to 0.0025 mm penetration (M scale is 0.00125 mm).

To perform a test, the unit is placed on the sample so that the presser foot is held firmly against the test surface. The spring pushes the indenter into the sample and the indicator displays the depth of penetration. A deeper indentation indicates that the material is soft, and consequently the result would be a low indicator reading. The Shore A and D test method are the most commonly used scales. The M scale uses a very low force spring and was developed to allow testing very small parts, such as o-rings that cannot be tested in the normal A scale. Because different materials respond to the test scales in different ways, there is no correlation between the different scales. Shore test methods are defined in the following standards: ASTM D 2240, DIN 53 505, ISO 7619 Part 1, JIS K 6253, ASKER, and C-SRIS-010 1 (now obsolete).

A density kit is used to determine the volume of an o-ring, and the measurements are usually made using an auxiliary liquid with a known density. In this case, water is used as the auxiliary liquid. The weight of the o-ring is measured in air and water before and after the dynamic test. The temperature of water (auxiliary liquid) is recorded to determine the density of water. The weight of the elastomer material in air (w_{air}) and water (w_{water}), along with the density of air (ρ_{air}) and water (ρ_{water}), is used to determine the volume of the elastomer material. The expression for computing volume (V) is shown in Equation 1. α is the weight correction factor 0.99985 to take the atmospheric buoyancy of the adjustment weight into account. Since the density of air does not vary significantly with temperature, ρ_{air} is set at a constant value of 0.0012 g/cm^3 . A density kit model ML-DNY-43 is used in combination with a balance model ML 104/03, as shown in Figure A-3.

$$V = \alpha \cdot \left[\frac{W_{air} - W_{water}}{\rho_{water} - \rho_{air}} \right] \rightarrow (1)$$



Figure A-3. Density Kit to Measure O-ring Volume

**APPENDIX B.
GC-MS SPECTRA**

The sample numbers (CL15-) for the used brake fluids from static soak tests are listed in Table B- 1 below. Figure B- 1 to Figure B- 18, shows the GC-MS spectra for neat brake fluids and overlays with used fluids from static soak tests.

Table B- 1. Sample Numbers of used Brake Fluids from Static Soak Tests

Sample ID	Description of the fluid
Neat HSF	Neat Silicone Brake Fluid
Neat SAE J1703	Neat SAE J1703 Fluid
CL15-8024	Used HSF containing SBR at 40°C
CL15-8025	Used SAE J1703 containing SBR at 40°C
CL15-8032	Used HSF containing SBR at ambient conditions
CL15-8033	Used SAE J1703 containing SBR at ambient conditions
CL15-8020	Used HSF containing Neoprene at 40°C
CL15-8021	Used SAE J1703 containing Neoprene at 40°C
CL15-8028	Used HSF containing Neoprene at ambient conditions
CL15-8029	Used SAE J1703 containing Neoprene at ambient conditions
CL15-8018	Used HSF containing EPDM at 40°C
CL15-8019	Used SAE J1703 containing EPDM at 40°C
CL15-8027	Used SAE J1703 containing EPDM at ambient conditions
CL15-8026	Used HSF containing EPDM at ambient conditions
CL15-8022	Used HSF containing Silicone at 40°C
CL15-8023	Used SAE J1703 containing Silicone at 40°C
CL15-8030	Used HSF containing Silicone at ambient conditions
CL15-8031	Used SAE J1703 containing Silicone at ambient conditions

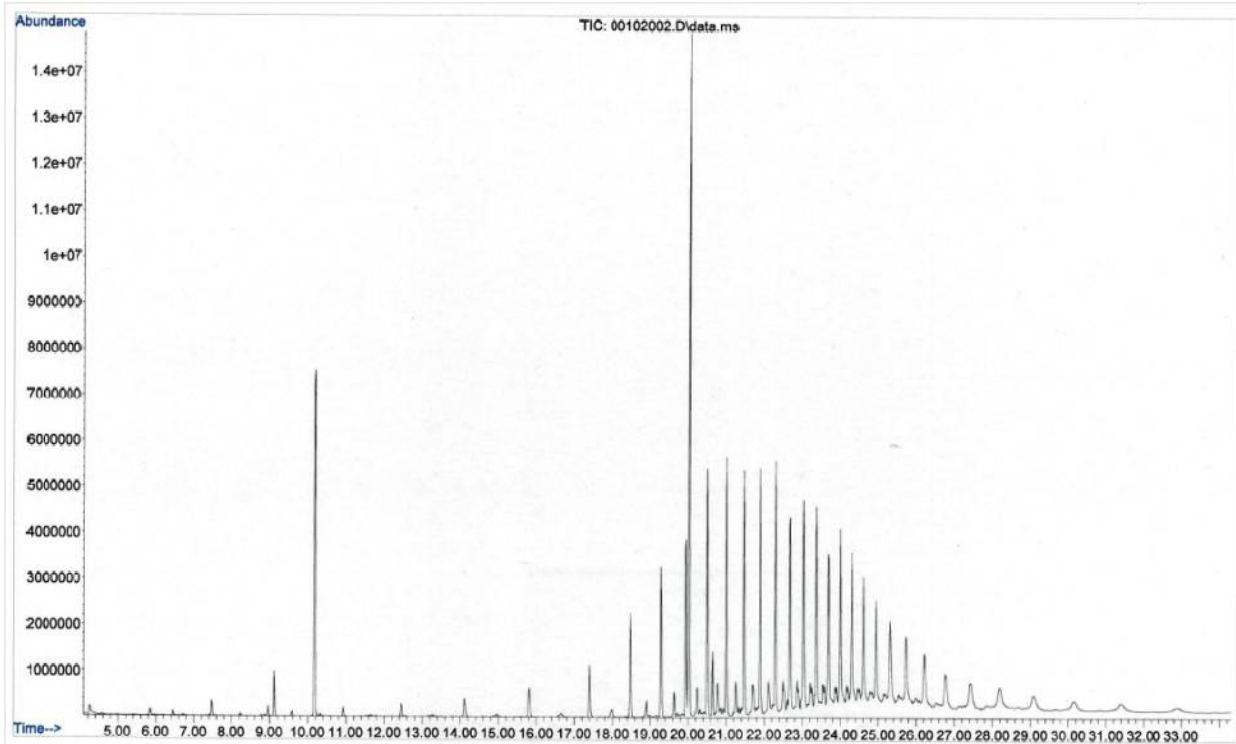


Figure B- 1. GC-MS Spectra for neat silicone brake fluid (HSF)

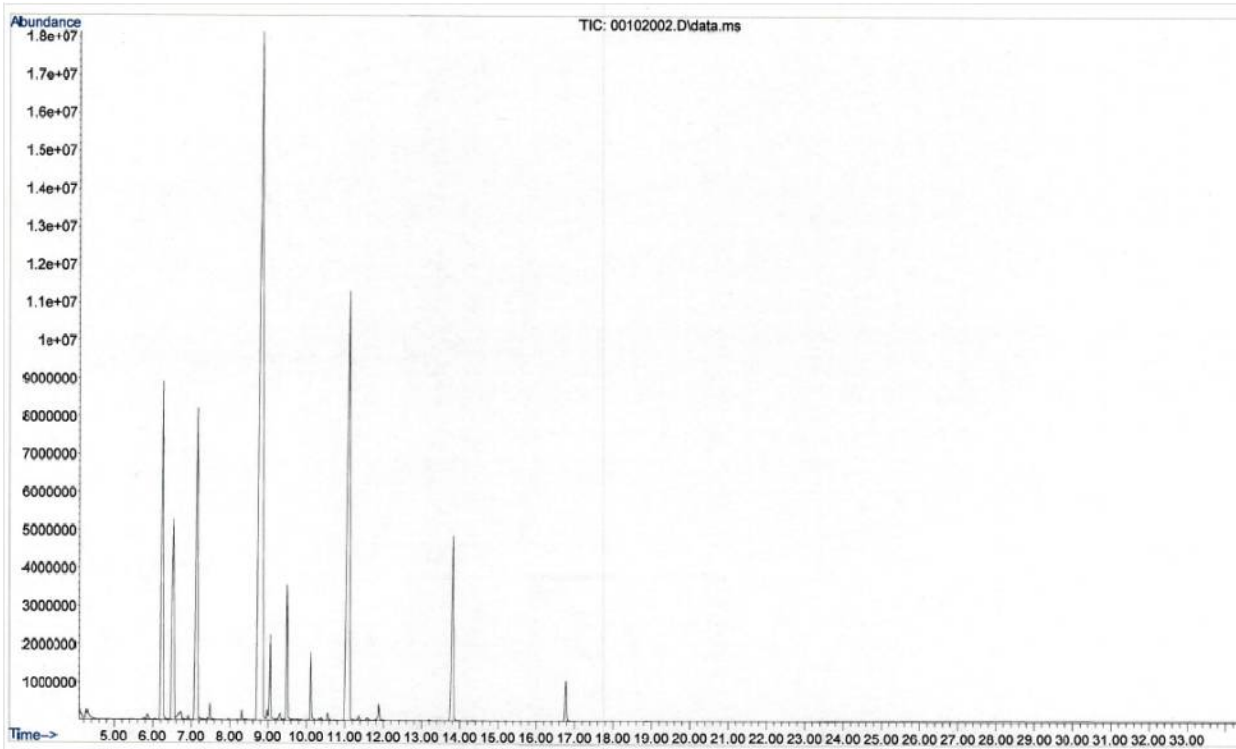


Figure B- 2. GC-MS Spectra for neat baseline brake fluid (SAE J1703)

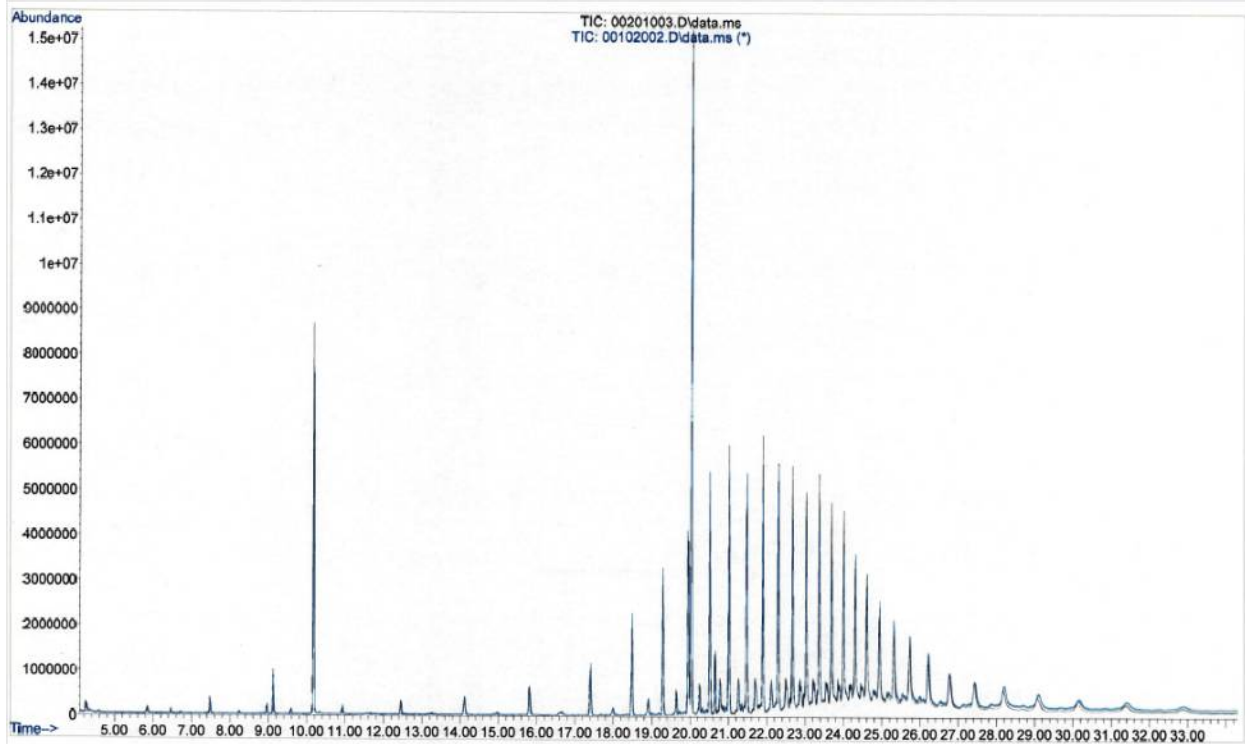


Figure B- 3. GC-MS Spectra for HSF containing EPDM at 40 °C

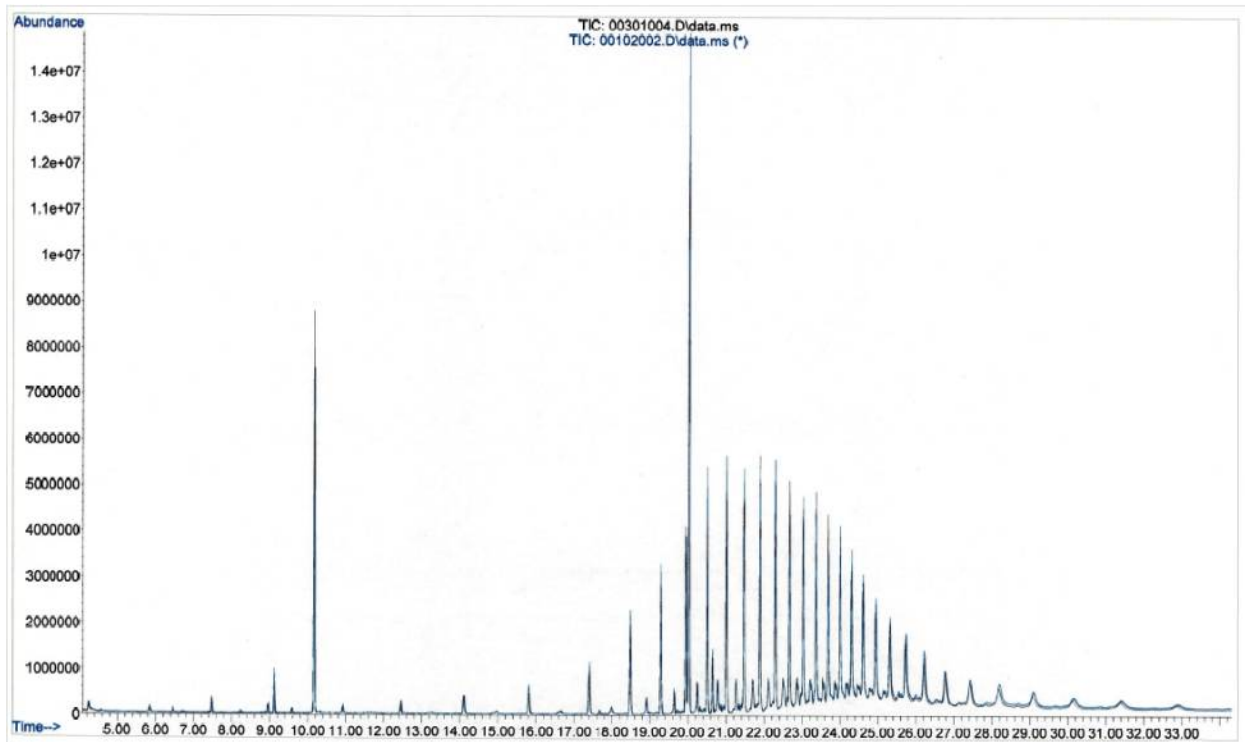


Figure B- 4. GC-MS Spectra for HSF containing Neoprene at 40 °C

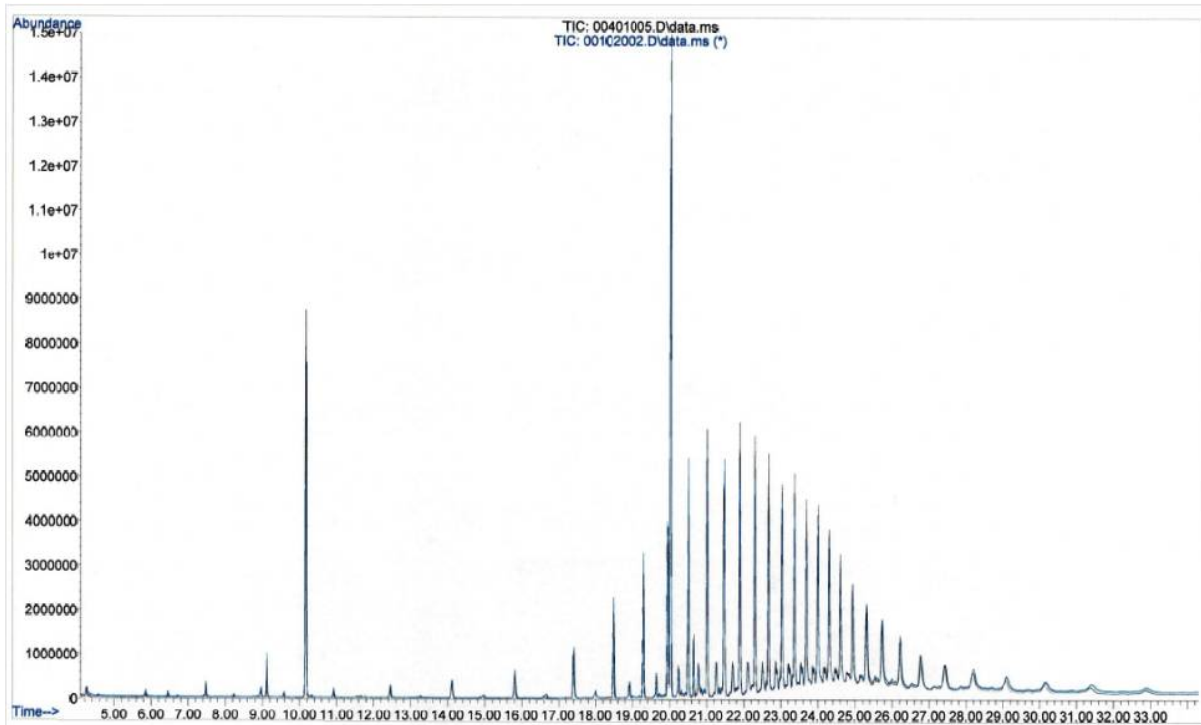


Figure B- 5. GC-MS Spectra for HSF containing Silicone at 40 °C

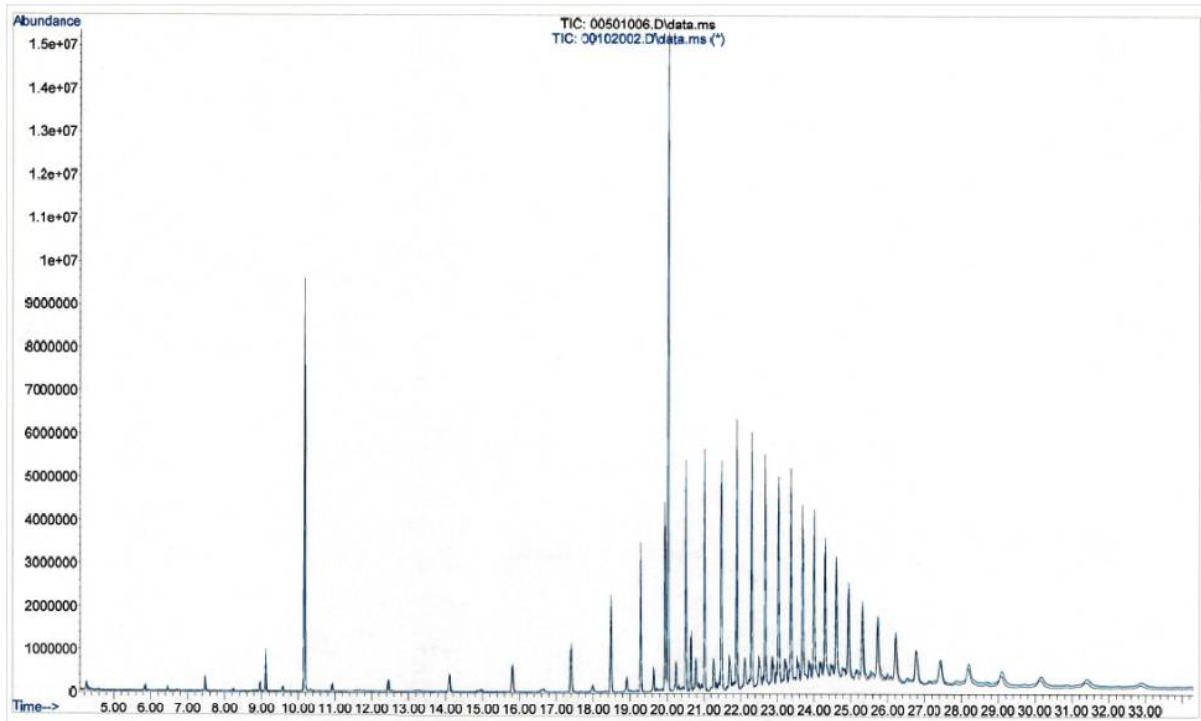


Figure B- 6. GC-MS Spectra for HSF containing SBR at 40 °C

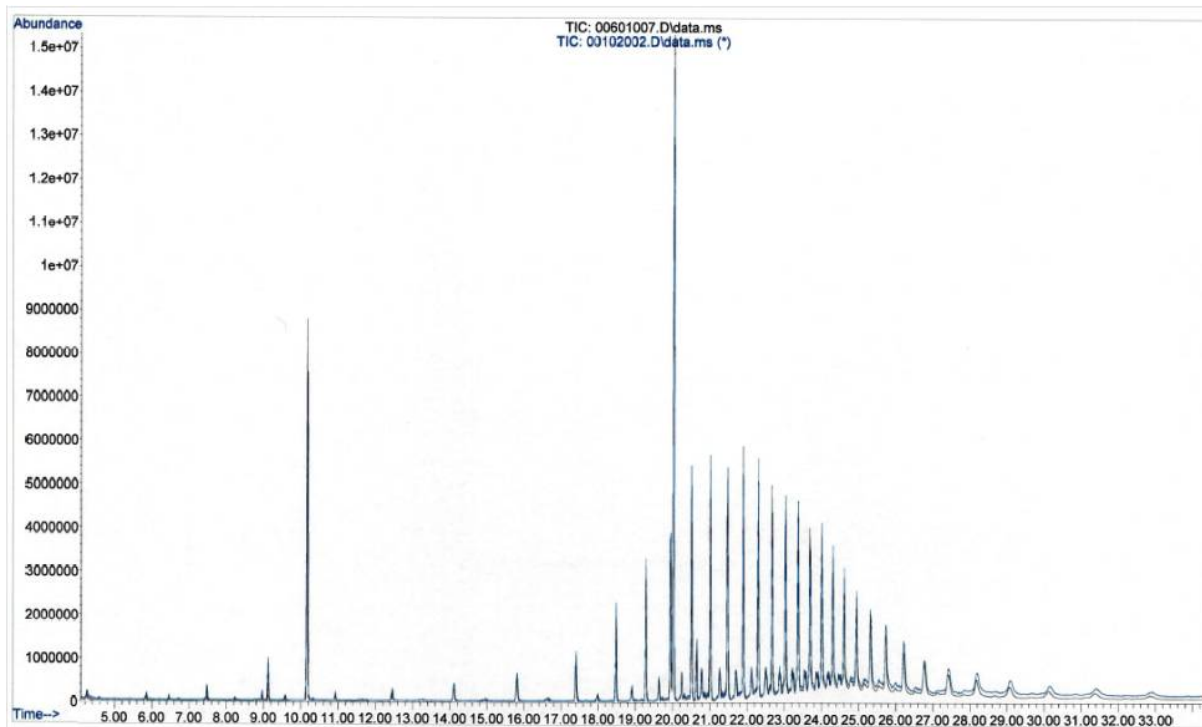


Figure B- 7. GC-MS Spectra for HSF containing EPDM at ambient conditions

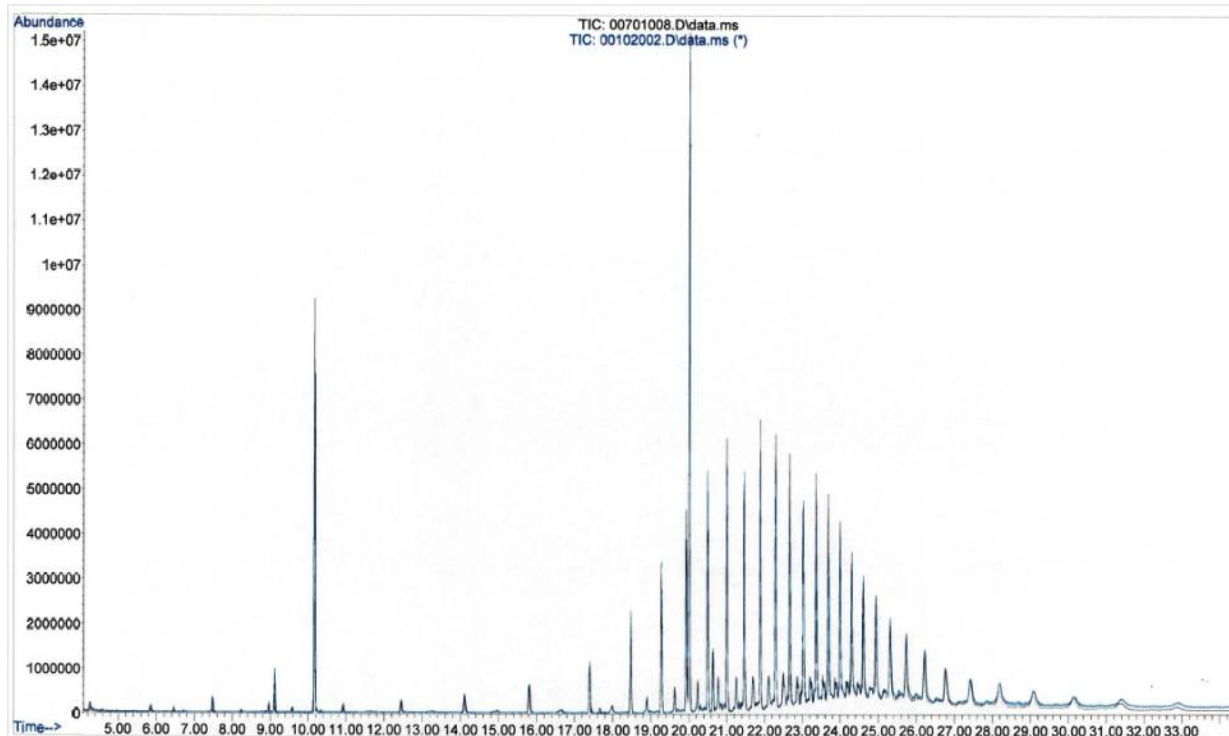


Figure B- 8. GC-MS Spectra for HSF containing Neoprene at ambient conditions

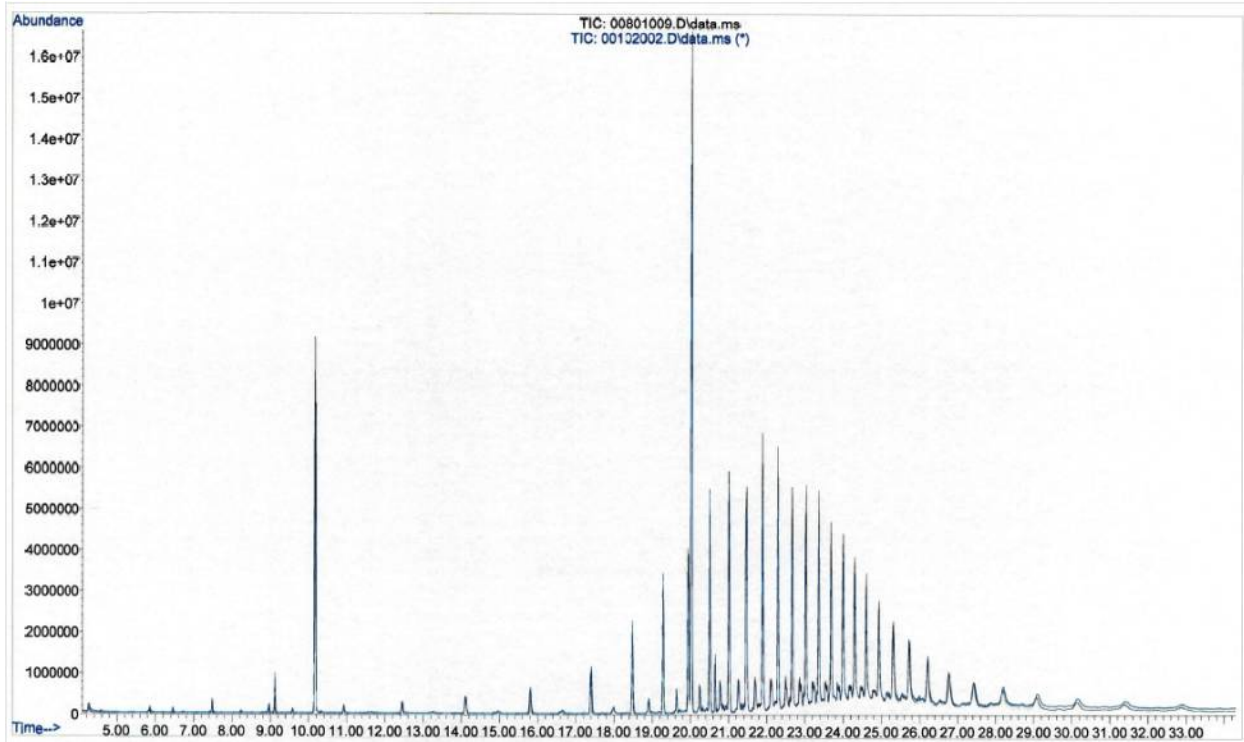


Figure B- 9. GC-MS Spectra for HSF containing Silicone at ambient conditions

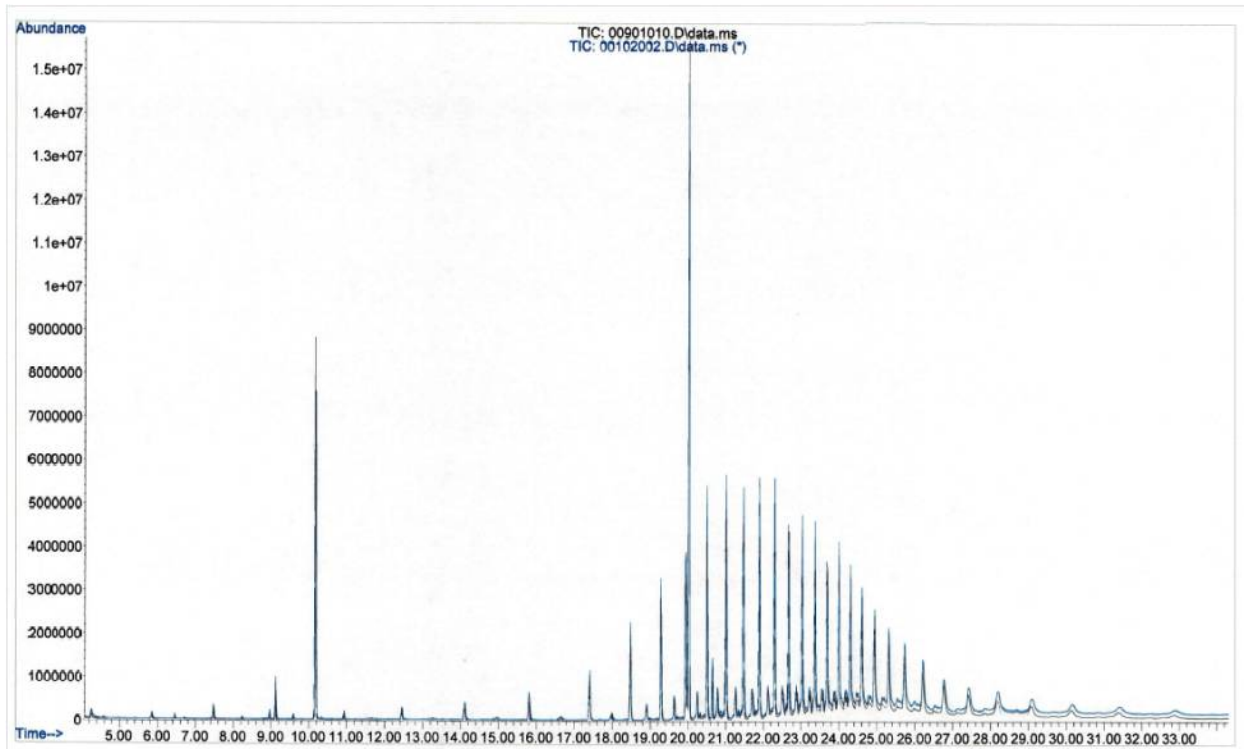


Figure B- 10. GC-MS Spectra for HSF containing SBR at ambient conditions

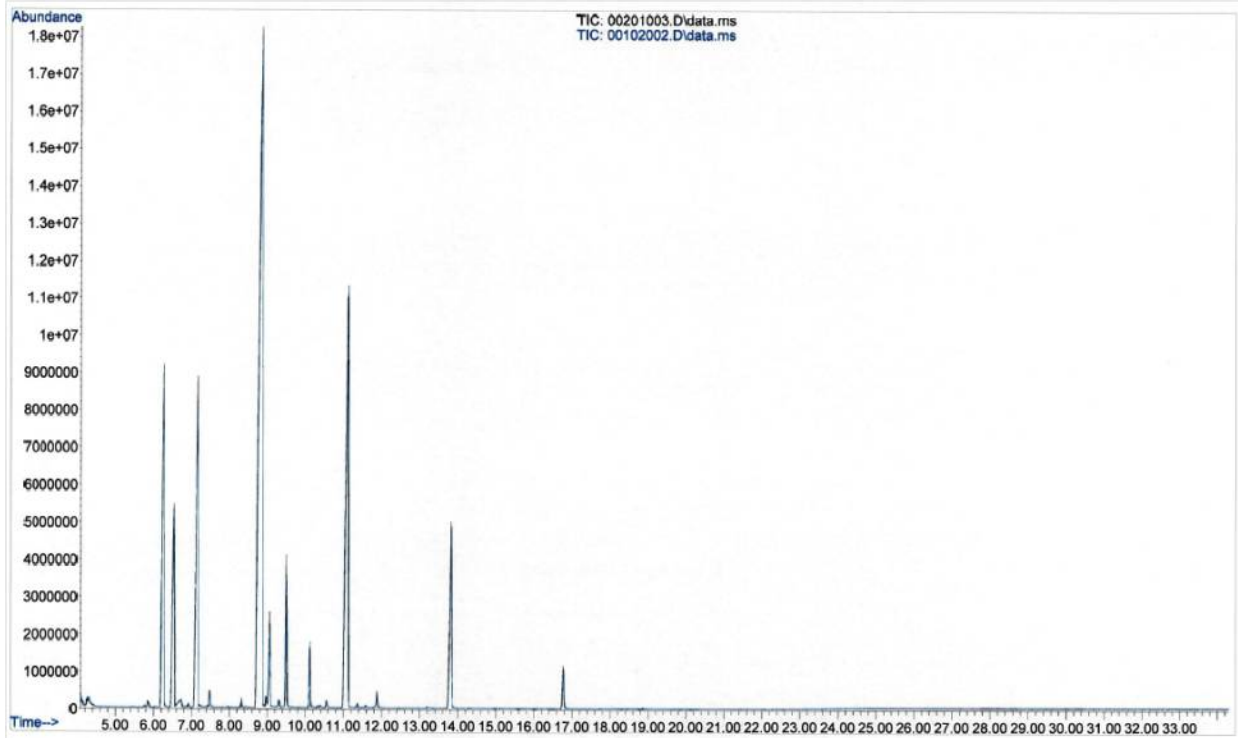


Figure B- 11. GC-MS Spectra for SAE J1703 fluid containing EPDM at 40 °C

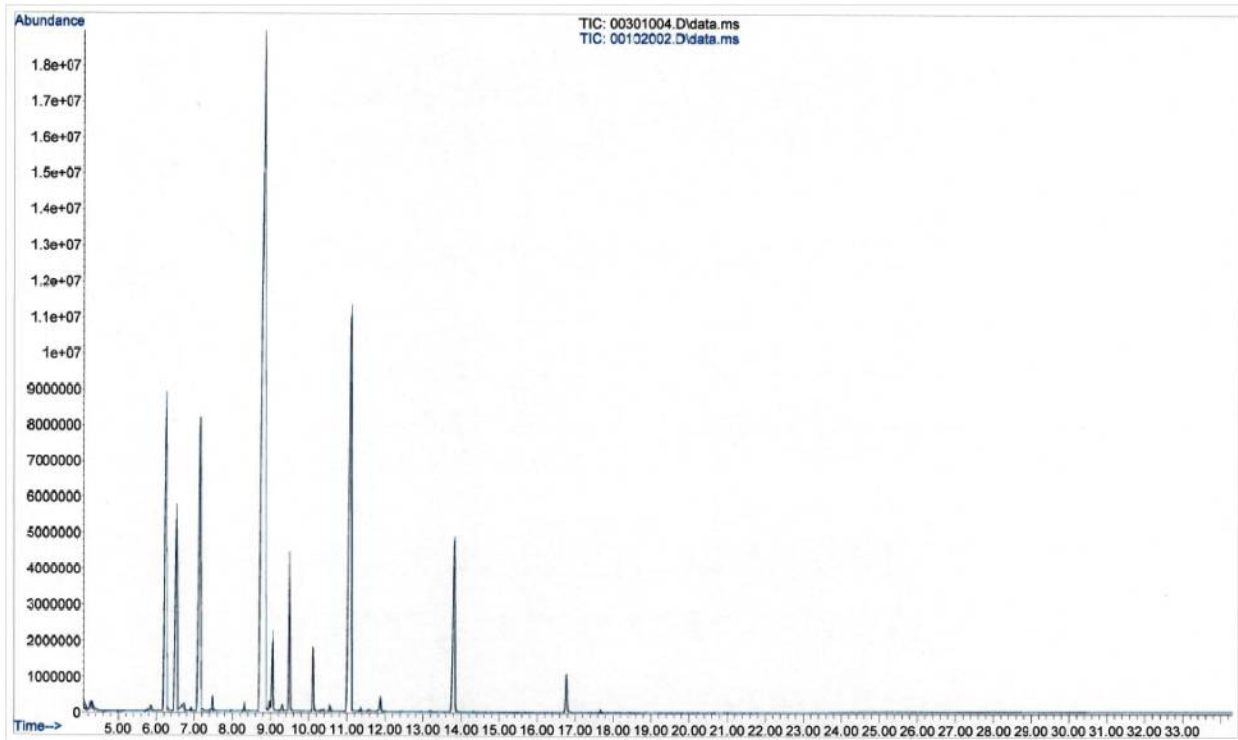


Figure B- 12. GC-MS Spectra for SAE J1703 fluid containing Neoprene at 40 °C

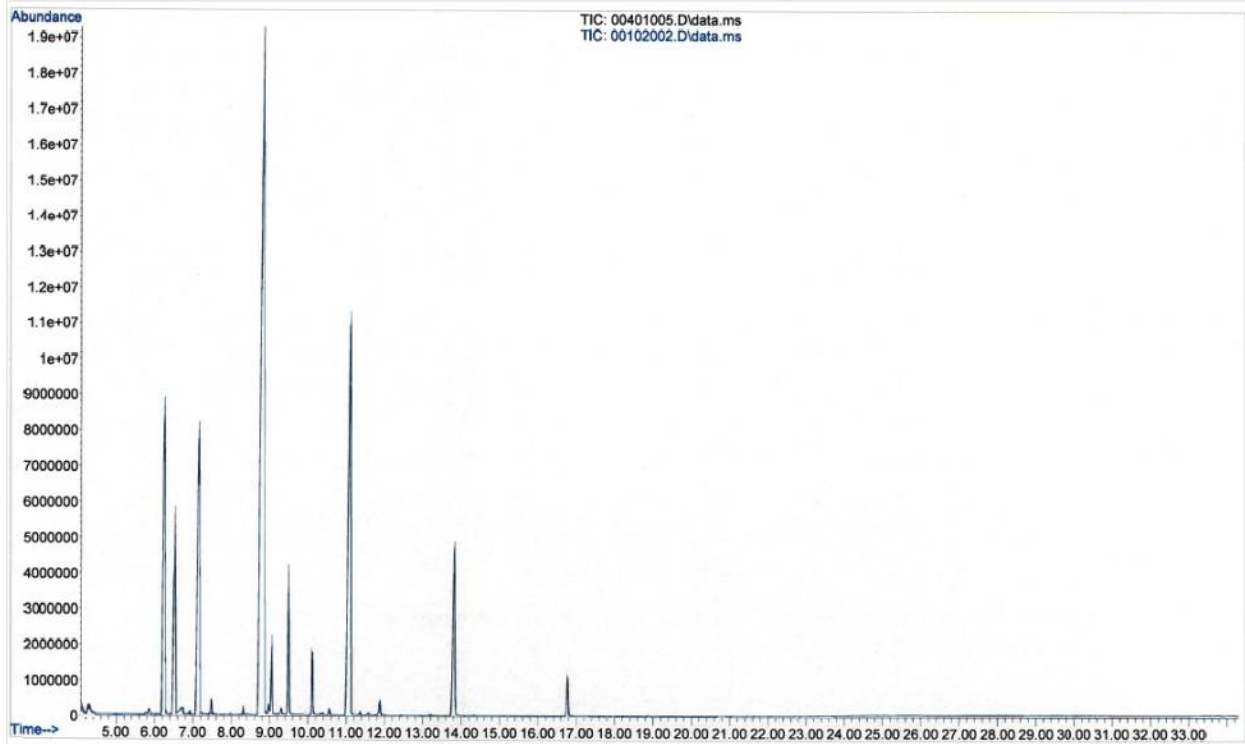


Figure B- 13. GC-MS Spectra for SAE J1703 fluid containing Silicone at 40 °C

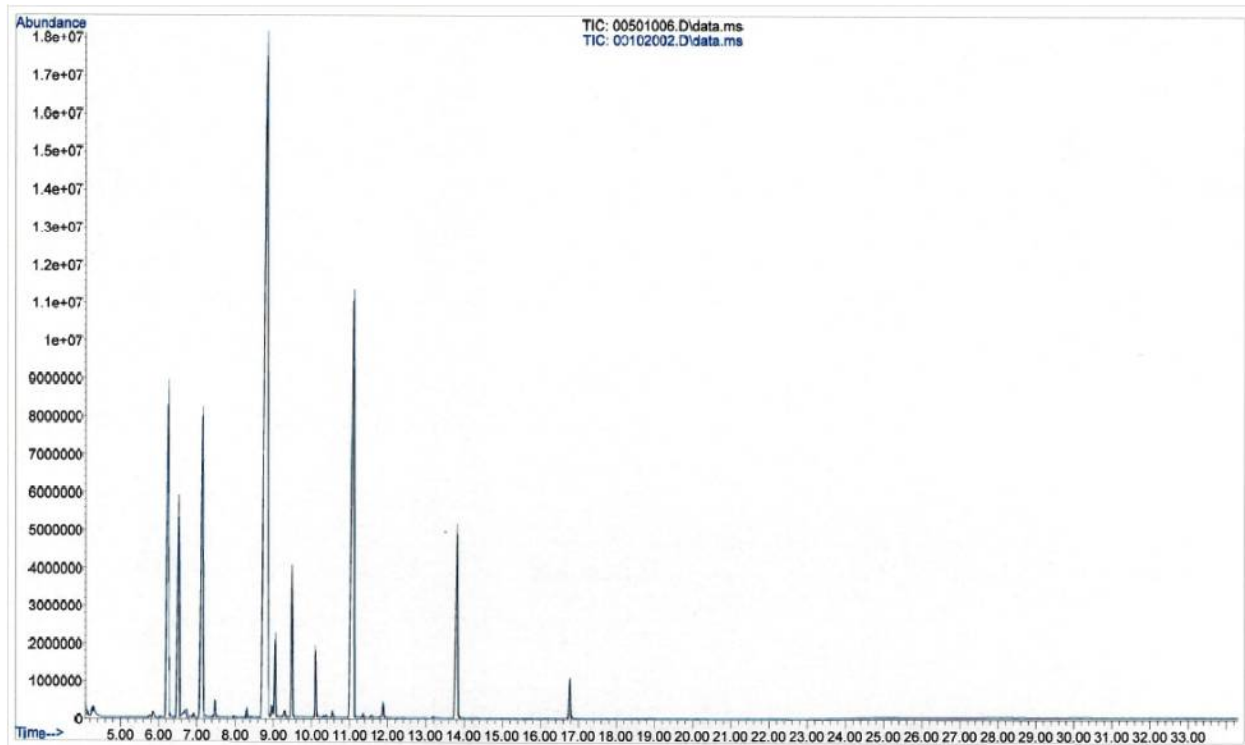


Figure B- 14. GC-MS Spectra for SAE J1703 fluid containing SBR at 40 °C

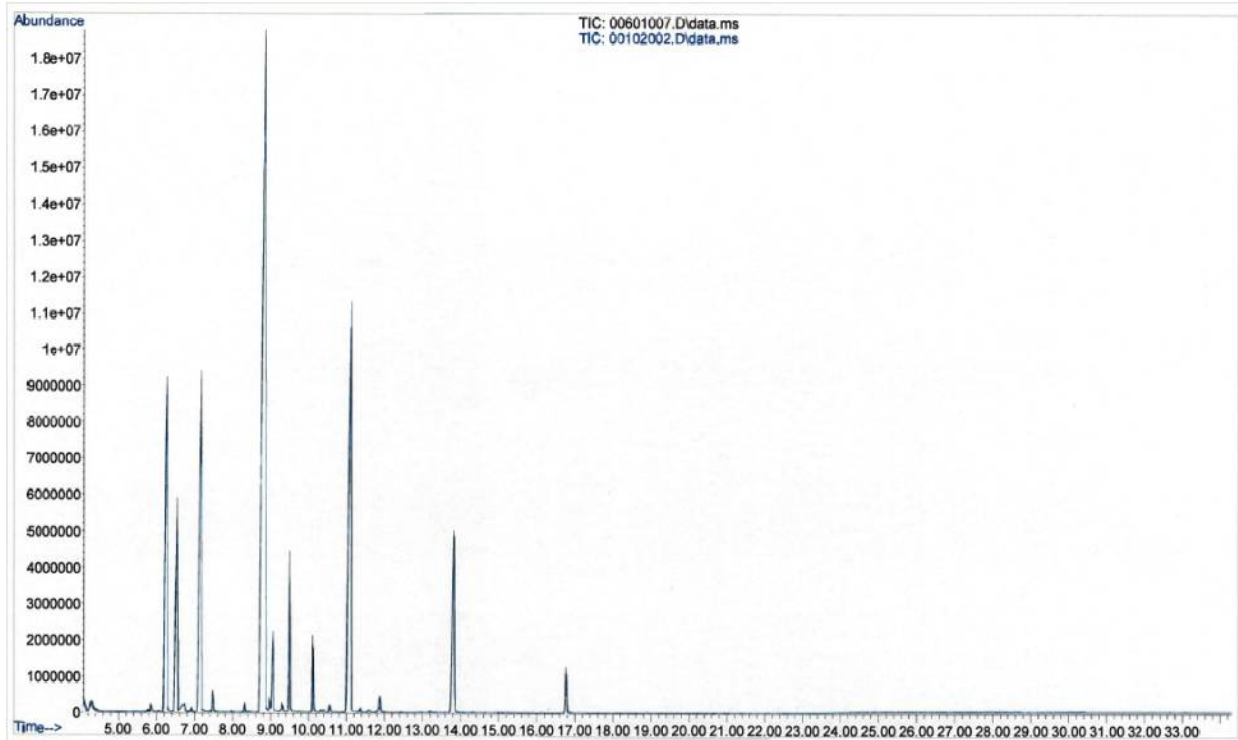


Figure B- 15. GC-MS Spectra for SAE J1703 fluid containing EPDM at ambient conditions

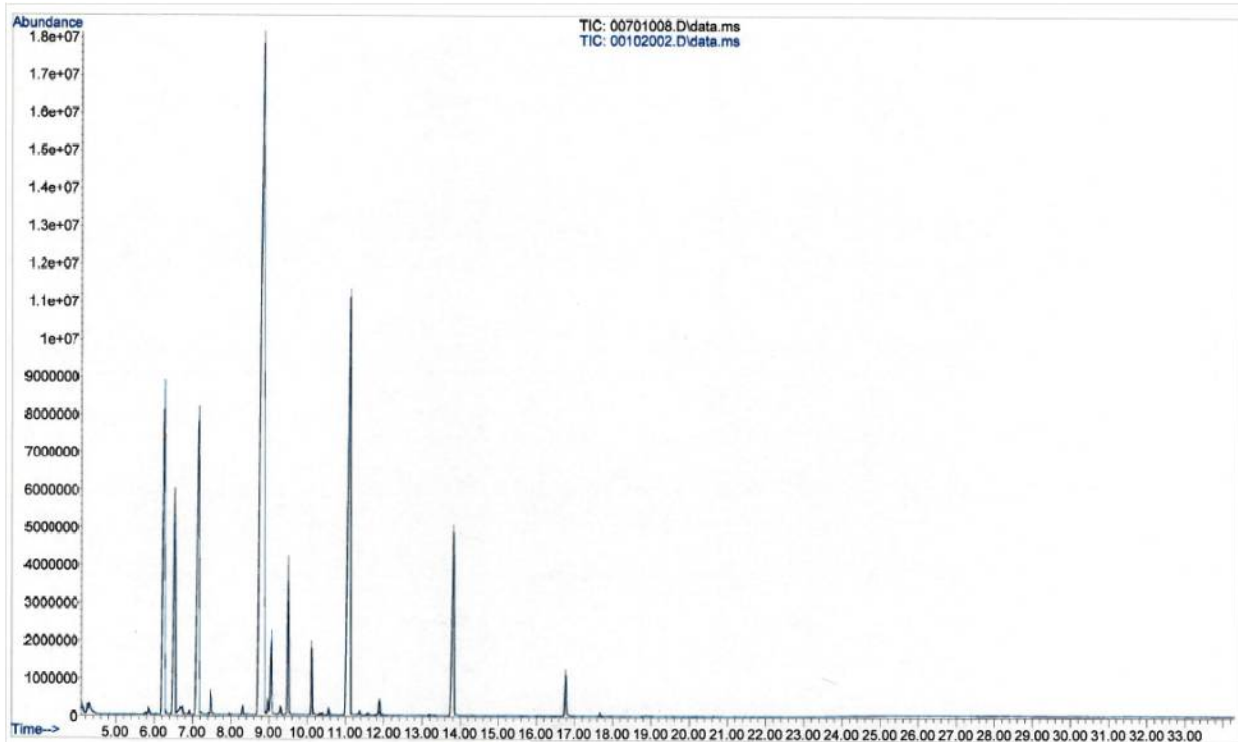


Figure B- 16. GC-MS Spectra for SAE J1703 fluid containing Neoprene at ambient conditions

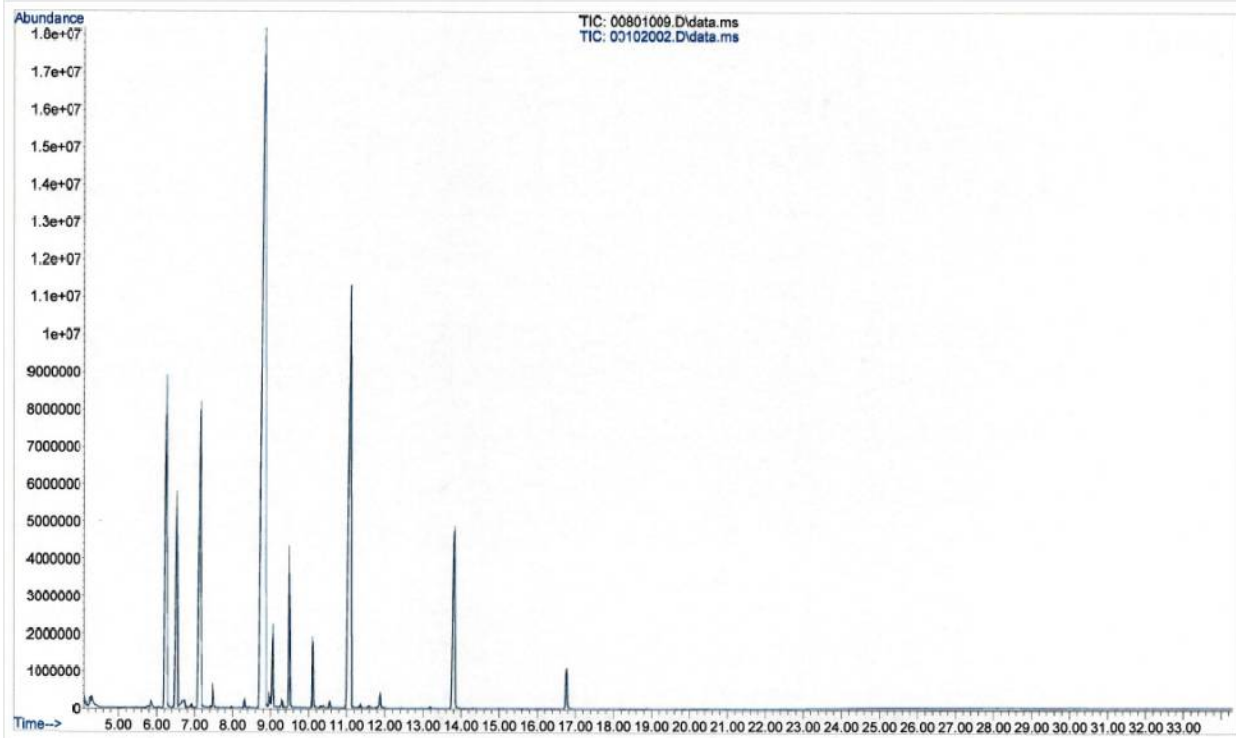


Figure B- 17. GC-MS Spectra for SAE J1703 fluid containing Silicone at ambient conditions

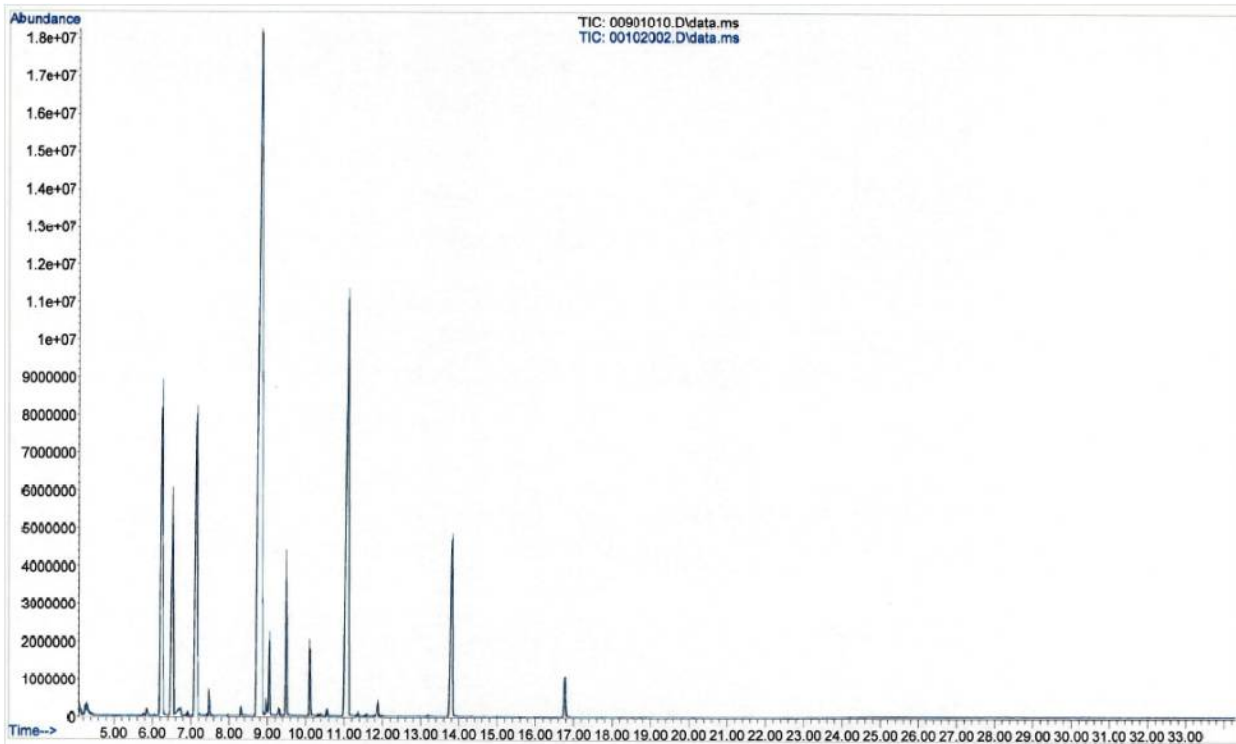


Figure B- 18. GC-MS Spectra for SAE J1703 fluid containing SBR at ambient conditions